Université de Montréal

Adenosine nucleotides identified in *Actinobacillus pleuropneumoniae* supernatant inhibit porcine reproductive and respiratory syndrome virus replication *in vitro*

Par

Abdulrahman F. Salmin

Département de biomédecine vétérinaire

Faculté de médecine vétérinaire

Mémoire présenté à la Faculté de médecine vétérinaire

en vue de l'obtention du grade de *Maîtrise ès sciences* (M. Sc.)

en sciences vétérinaires, option pharmacologie

Août 2021

Université de Montréal

Faculté de médecine vétérinaire

Ce mémoire intitulé

Adenosine nucleotides identified in *Actinobacillus pleuropneumoniae* supernatant inhibit porcine reproductive and respiratory syndrome virus replication *in vitro*

Présenté par

Abdulrahman F. Salmin

A été évalué par un jury composé des personnes suivantes :

M. Marcio Carvalho Costa

Président-rapporteur

M. Francis Beaudry

Directeur de recherche

M. Carl A. Gagnon

Codirecteur

M. Mario Jacques

Codirecteur

M. Younès Chorfi

Membre du jury

Résumé

Le virus du syndrome reproducteur et respiratoire porcin (VSRRP) est un pathogène ayant d'énormes conséquences pour les producteurs porcins. Il est la cause d'une des maladies les plus coûteuses à l'industrie au Québec et, à ce jour, il n'y a aucun traitement efficace commercialement disponible contre le virus. Il a été précédemment démontré que le surnageant de culture de bactéries *Actinobacillus pleuropneumoniae (App)* - l'agent causant la pleuropneumonie porcine - possède une activité antivirale *in vitro* contre le VSRRP. Ces études ont déterminé que cette activité était en fait médiée par des métabolites excrétés par les bactéries d'*App*, résistants à la chaleur et de faible poids moléculaire.

Cependant, l'identité de ces métabolites demeurait inconnue, menant ainsi aux objectifs de ce projet : (I) produire un surnageant actif d'*App*; (II) caractériser et identifier les métabolites actifs utilisant la spectrométrie de masse à haute résolution (HRMS); (III) tester et évaluer l'activité antivirale des composés purifiés. De nombreux métabolites de nucléotides de l'adénosine en haute concentration dans le surnageant d'*App* ont ainsi été identifiés par HRMS. Pour confirmer l'effet antiviral du surnageant et des métabolites actifs identifiés, un modèle d'infection de cellules SJPL permissives au VSRRP et de l'imagerie à immunofluorescence ont été employés. Les métabolites ont en effet montré une inhibition de la réplication du VSRRP dans les cellules et leurs mécanismes d'actions sont déjà bien répertoriés; soit l'inhibition des polymérases d'ARN cellulaire et virale par la forme de triphosphate de nucléoside, ainsi que l'arrêt de synthèse des acides nucléiques lors de la réplication virale. Cette étude propose donc de nouvelles ouvertures, basé sur les mécanismes d'actions cellulaires responsables de l'effet antiviral, pour développer des traitements préventifs contre le VSRRP.

Mots clés : Virus du syndrome reproducteur et respiratoire porcin (VSRRP), *Actinobacillus pleuropneumoniae (App)*, effet antiviral, spectrométrie de masse, immunofluoresence, phosphate d'adénosine

Abstract

Porcine reproductive and respiratory syndrome virus (PRRSV) is one of the most devastating viruses in the swine industry. It causes major economic losses worldwide on an annual basis. To date, there has not been an effective treatment for this virus. Previous studies conducted in our group have shown that the culture supernatant of *Actinobacillus pleuropneumoniae (App)*, the causative agent of porcine pleuropneumonia, possesses an antiviral activity *in vitro* against PRRSV. These studies have shown that the antiviral activity was mediated by small molecular weight, heat resistant metabolites present in the *App* supernatant ultrafiltrates.

However, the identity of those metabolites remained unknown, which led us to the objectives of this study: (I)generate an active supernatant; (II)characterize and identify the active metabolites using high resolution mass spectrometry; (III)evaluate the antiviral activity of the purified compounds following identification. In this study we utilized a virus infection model using SJPL cells and immunofluorescence imagery to confirm the antiviral activity of the *App* supernatant as our first approach. Subsequently, using high resolution mass spectrometry we identified several adenosine nucleotide metabolites present in *App* supernatants in high concentrations. Following testing, we revealed that several adenosine nucleotide metabolites inhibit PRRSV replication in SJPL cells. Interestingly, the antiviral mechanism of action of adenosine nucleotide analogs is already known. The nucleoside triphosphate form functions by inhibiting cellular and viral RNA polymerases and during viral RNA replication, incorporates nucleoside analogs into nascent RNA chains resulting in termination of nucleic acid synthesis. This study may suggest new approaches to develop prophylactic treatment for PRRSV.

Keywords: Porcine reproductive and respiratory syndrome virus (PRRSV), *Actinobacillus pleuropneumoniae (APP)*, antiviral effect, mass spectrometry, immunofluorescence assay (IFA), adenosine phosphates.

Table of contents

List of tables

List of figures

List of acronyms and abbreviations

aa: Amino acids

ACC1: Acetyl-CoA carboxylase 1

AMPK: 5'-AMP-activated protein kinase

App: *Actinobacillus pleuropneumoniae*

AppΔapxICΔapxIIC: Mutant *App* strain

ATP: Adenosine triphosphate

cAMP: Cyclic adenosine monophosphate

CMI: Cell mediated immune response

CoA: Coenzyme A

DDA: Data dependant acquisition

DENV-2: Dengue-2 virus

DIM: 3,3'-Diindolylmethane

EAV: Equine artiritis virus

EBOV: Ebola virus

EU: European

FDAs: Food and drug administrations

GP: Glycoproteins

gRNA: Viral genomic RNA

HCV: Hepatitis C virus

HMVEC: Human lung microvascular endothelial cells

HPLC-MS: High performance liquid chromatography tandem mass spectrometry

HP-PRRSV: Highly pathogenic porcine reproductive and respiratory syndrome virus

HRAM: High resolution accurate mass spectrometry

IFA: Immunofluorescence assay

IFNα: Interferon alpha

LDV: Lactate dehydrogenase-elevating virus

LPS: Lipopolysaccharides

m/z: Mass to charge ratio

MERS-CoV: Middle east respiratory syndrome coronavirus

MOI: Multiplicity of infection

mRNA: Messenger RNA

MS: Mass spectrometer

NA: North American

NAb: Neutralizing antibodies

NAD: Nicotinamide adenine di-nucleotide

NK cells: Natural killer cells

NOD1: Nucleotide-binding oligomerization domain-containing protein 1

NOD2: Nucleotide-binding oligomerization domain-containing protein 2

nsp: non-structural protein

NTPase: Nucleoside-triphosphatase

ORFs: Open reading frames

PAM: Porcine alveolar macrophages

PCV2: Porcine circovirus type 2

PD: Pharmacodynamics

pi: Post infection

PK: Pharmacokinetics

PRDC: Porcine respiratory disease complex

ProTide: Prodrug nucleotide

PRRS: Porcine reproductive and respiratory syndrome

PRRSV: Porcine reproductive and respiratory syndrome virus

RdRp: RNA-dependant RNA polymerase

RNA: Ribonucleic acid

RT-qPCR: Quantitative reverse transcription polymerase chain reaction

SAR: Structure activity relationship

SARS-CoV : Severe acute respiratory syndrome coronavirus

sgRNA: Subgenomic RNA

SHFV: Simian hemorrhagic fever virus

SJPL: Saint Jude porcine lung cells

TNF-α: Tumor necrosis factor alpha

UV: Ultraviolet

WNV: West Nile virus

YFV: Yellow fever virus

Dedicated to my family

Acknowledgments

I would like to express my gratitude to everyone who has mentored me, encouraged me and assisted me through my two-year journey. Words cannot describe the appreciation that I have for my director Dr. Francis Beaudry, for offering me this great opportunity. I would like to thank him for his patience with me, his kindness and devotion. I have learnt a lot under your instruction and have managed to expand my skillset and perform tasks I never thought I would be able to perform.

I would like to extend my thanks to my co-directors, Dr. Gagnon and Dr. Jacques whom this work wouldn't have been possible if not for the research that they conducted in previous years. A special thanks to Dr. Gagnon for teaching me a great deal about virology, and for opening his lab to me. I am grateful for the organizations who financed this project: Natural Sciences and Engineering Research Council of Canada (NSERC), Canadian Swine Research and Development Cluster (CSRDC), Les éleveurs de porcs du Québec, Probiotech international Inc, Centre de diagnostic vétérinaire de l'Université de Montréal and Illumina Inc, as well as the Centre de recherche en infectiologie porcine et avicole (CRIPA) and Groupe de recherche en pharmacologie animale du Quebec (GREPAQ).

I appreciate and am thankful to all the members of the laboratories whom I have had the pleasure of working with, starting with Dr. Provost who has taught me much and has been very patient and enlightening, a special thanks to my colleague and friend Marie-Jeanne who has assisted me in numerous occasions. Grateful to Josée Labrie, research assistant in Dr. Mario Jacques' laboratory for providing us with the *Actinobacillus pleuropneumoniae* we needed for this project.

Lastly but not least, I would like to express my gratitude to my family, my parents and my sisters who believed in me and constantly pushed me to achieve better and who are always there for me when I need them.

INTRODUCTION

Porcine reproductive and respiratory syndrome (PRRS) is a worldwide endemic disease causing significant economic losses in pig-producing countries. In sows, PRRS is characterized by reproductive failure, late-term abortions, increased numbers of stillborn fetuses, and/or premature and weak piglets [1-5]. During PRRS disease, there is an increase in the morbidity and mortality of both growing and finishing pigs, this is owed to the severe respiratory disease and poor growth performance observed [6, 7]. The causative agent, porcine reproductive and respiratory syndrome virus (PRRSV), belongs to the family *Arteriviridae* of the *Nidovirales* order. PRRSV is an enveloped single-stranded positive sense RNA virus of approximately 15 kb in length that encodes at least 11 open reading frames (ORFs) [8]. Like numerous RNA viruses, PRRSV genome heterogeneity represents the main obstacle to effective prevention and control of the disease through vaccination [9].

In pigs, the term "Porcine Respiratory Disease Complex" (PRDC) is often used to describe coinfections involving viruses such as swine Influenza A Virus (swIAV), Porcine Reproductive and Respiratory Syndrome Virus (PRRSV), and Porcine circovirus type 2 (PCV2) as well as bacteria like *Actinobacillus pleuropneumoniae* (*App*), *Mycoplasma hyopneumoniae* and *Bordetella bronchiseptica* [10]. *App* is the causative agent of porcine pleuropneumonia, a disease responsible for major economic losses in the swine industry worldwide. In recent years multiple *in vitro* studies have been done in our group to investigate the interactions between *App* and PRRSV using multiple cell lines, namely the St Jude porcine lung (SJPL), MARC-145 and porcine alveolar macrophage (PAM) cell lines [11-14].

The investigations were launched since co-infections are likely more common than reported in the field, and that a primary infection with a viral or bacterial pathogen may enhance the infectious potential of a secondary pathogen. Interestingly, it was unexpectedly observed that *App* culture supernatants have strong antiviral activity against the porcine reproductive

and respiratory syndrome virus (PRRSV), during *App*-PRRSV co-infections of SJPL cells [12]. A more recent published study confirmed the *App* culture supernatant antiviral effect [13]. The antiviral effect against PRRSV was also observed in PAMs, the target cells of PRRSV during porcine infection [13]. It was also reported that *App* inhibits PRRSV by inducing cell cycle arrests in the G2/M phase of SJPL cells [14].

These studies uncovered that small molecular weight, heat-resistant metabolites present in *App* supernatant ultrafiltrates (< 1 kDa) and not LPS (extracted whole molecules) or peptidoglycan fragments (i.e. NOD1 and NOD2 ligands) were responsible for the *App* antiviral activity [12]. However, prior experiments using a low-resolution mass spectrometer (MS) instrument were unsuccessful in identifying potential candidates with absolute certainty.

In the present thesis, we hypothesize that the culture supernatant of *App* contains specific unidentified molecules which induce an antiviral activity against PRRSV in SJPL cells *in vitro.* The aim of the current study is to (i) generate an active *App* supernatant, (ii) identify the unknown metabolites using high resolution mass spectrometry techniques and (iii) assess the antiviral activity of the purified compounds following identification. The findings of this study may unveil novel therapeutic or prophylactic approaches to combat and treat PRRSV infection.

Literature review

1. Porcine Respiratory Disease complex

Pigs are susceptible to a plethora of diseases which can be difficult to diagnose and treat; these diseases can cause massive economic losses in the production sector. One of such diseases is Porcine respiratory disease complex (PRDC).

PRDC is a multifactorial disease affecting pigs. Pigs are often colonized by more than one bacterial/viral species during respiratory tract infection [15]. *Actinobacillus pleuropneumoniae (App)* and porcine reproductive and respiratory syndrome virus (PRRSV) are two pathogens that are frequently involved in PRDC [15]. Other major etiological agents involved in PRDC include Porcine circovirus type 2(PCV2), *Haemophilus parasuis,* and Swine influenza virus as displayed in Table 1 [15]. PRDC is characterized as pneumonia of multiple etiologies causing clinical disease and failure to gain weight later in the finishing process (15 to 20 weeks of age) [16]. Common clinical signs of PRDC include lethargy, anorexia, fever, nasal and ocular discharges, coughing and labored breathing [16]. Additional non-infectious causes such as management and environmental factors play a significant role in the contribution towards PRDC, by increasing the transmission, spread of pathogens and creating unfavorable conditions which result in increased stress for the animal or damage to the respiratory tract [16]. Overcrowding and a lack of proper ventilation can lead to overheating or chilling, increased stress, and escalation of ammonia and dust levels which have a negative impact on the respiratory tract defenses [16]. Current treatments for PRDC vary in accordance with the pathogens that are involved in the infection, a combination of vaccines and antibiotics is conventionally administered, however the efficacy of the current treatment models have been less than satisfactory [17]. Specific measures preventing PRDC infection can be implemented by enhancing management practices such as improving ventilation and preventing overcrowding.

Table 1: Major etiological agents of PRDC (* are key agents in PRDC) [15]

Agent	Type	Primary/Secondary Infection
PRRSV*	Virus	Primary
Porcine Circovirus Type 2*	Virus	Primary
Swine Influenza Virus*	Virus	Primary
Porcine Respiratory Coronavirus	Virus	Primary
*Mycoplasma hypopneumoniae**	Bacteria	Primary
*Actinobacillus pleuropneumoniae**	Bacteria	Primary
*Haemophilus parasuis**	Bacteria	Primary or secondary
Bordetella bronchiseptica	Bacteria	Primary
Streptococcus suis	Bacteria	Secondary
Pasteurella multocida	Bacteria	Secondary
Actinobacillus suis	Bacteria	Primary
Salmonella enterica Cholerasuis	Bacteria	Primary
Ascaris suum	Worms	Primary
Metastrongylus apri	Worms	Primary

2.Porcine reproductive and respiratory syndrome virus

Clinical outbreaks of porcine reproductive and respiratory disease (PRRS) were first reported in the late 1980's in the USA; similar clinical outbreaks were reported in Germany in 1990 and were widespread throughout Europe by 1991 [18]. However, the etiology of the disease remained unknown until 1991. In fact, the etiologic agent, porcine reproductive and respiratory syndrome virus (PRRSV) was identified in 1991 by investigators in the Netherlands and the USA [19, 20]. Since the 1990's PRRS has been an economically important disease around the globe; it has been estimated to cost the swine industry approximately US$ 560 million annually in USA alone [18, 21]. PRRSV emerged almost simultaneously in North America (genotype 2) and Western Europe (genotype 1) in the late 1980s and early 1990s. However, the virus strains that

originated from the two continents are strikingly different, with only 55–70% nucleotide identities [22, 23]. The evolutionary distance between the two lineages has led to the hypothesis that these two lineages have evolved separately from a very distant common ancestor [24]. Major events in PRRSV diversity were the emergence of an atypical variant that appeared in mid-1990s and the sudden appearance in 2001 of a novel strain named MN184 in the USA [25-27], the notable Type 2 highly pathogenic PRRSV (HP-PRRSV) in 2006 in China and subsequently most of Asia [28], and the demonstration of enhanced pathogenicity of the Type 1 Lena strain [29].

2.1 Clinical signs and symptoms

As its name implies, PRRS is characterized by severe disorders related to breeding stock such as premature births or abortions and disorders of the respiratory tract [30-33]. The incubation period of the disease is variable and ranges from a few days to over a month. Symptoms are not always perceptible, however, its highly dependent on the virulence of the PRRSV strains as well as the age and the immune status of the infected pigs [21, 32]. The size of the herd and the sanitary conditions of the farms are also important factors in the spread of the virus and disease. Reproductive and respiratory disorders may lead to several other complications such as eating disorders (anorexia) as well as agalactia and lethargy with or without cyanosis [21, 31, 32, 34].

2.2 Epidemiology

In infectiology, transmission is the passing of a pathogen causing communicable disease from an infected host individual or group to a particular individual or group, regardless of whether the other individual was previously infected [35].There are several modes of transmission, however, we will focus on the transmission modes that are adopted by PRRSV which include different direct and indirect routes outlined in Table 2 below [18].

With respect to direct routes of transmission infections following oral or nasal contact are the most common, due to the proximity of the pigs [36]. Vertical transmission during mid- to late-

gestation has also been reported as well as during nursing [30, 37]. Horizontal transmission has been reported following direct contact between infected animals and naïve animals [38], as well as transmission via semen of infected boars [18].

In the past years, several modes of indirect transmission have been identified [18, 39], however, several studies have demonstrated that certain intervention strategies such as the use of protocols, disposable gear and disinfectants substantially reduce the mechanical spread of the virus [40].

Table 2: Direct and indirect routes of PRRSV transmission

Direct routes	Indirect routes
Contact with body excretions and secretions (blood, semen, saliva, feces, aerosols, milk, and colostrum)	Fomites (boots and coveralls specifically)
Vertical transmission from sows to piglets	Needles and transport vehicles
Horizontal transmission through direct contact and through semen	Insects and aerosols

2.3 Taxonomy

Both PRRSV-1 and PRRSV-2 belong to the genus *Porarterivirus*, one of the five genera established within the family *Arteriviridae*, placed with the families *Mesoniviridae*, *Roniviridae* and *Coronaviridae* in the order nidovirales. The nidovirus order constitutes a group of single-stranded positive-sense RNA viruses, including equine arteritis virus (EAV), lactate dehydrogenase-elevating virus (LDV) of mice and simian hemorrhagic fever virus (SHFV) [41]. These viruses share a hallmark replication/transcription strategy, similar genomic organization, and a defining set of genetic elements, but differ in host species, range, disease phenotype, virion morphology, cellular tropism, genomic size and encoded content [42].

2.4 General structure

The PRRSV is an enveloped, single-stranded, positive sense RNA virus, approximately 50–65 nm in diameter [18]. The N proteins that constitute PRRSV form a helical capsid 20 to 30 nm in diameter [43]. The nucleocapsid is predominantly composed of N proteins. It is surrounded by a

viral envelope containing various structural proteins such as GP2, E, GP3 and GP4.This envelope also presents other proteins such as GP5 and M [41]. Figure 1 below shows the general structure of PRRSV, and the localization of the various proteins mentioned.

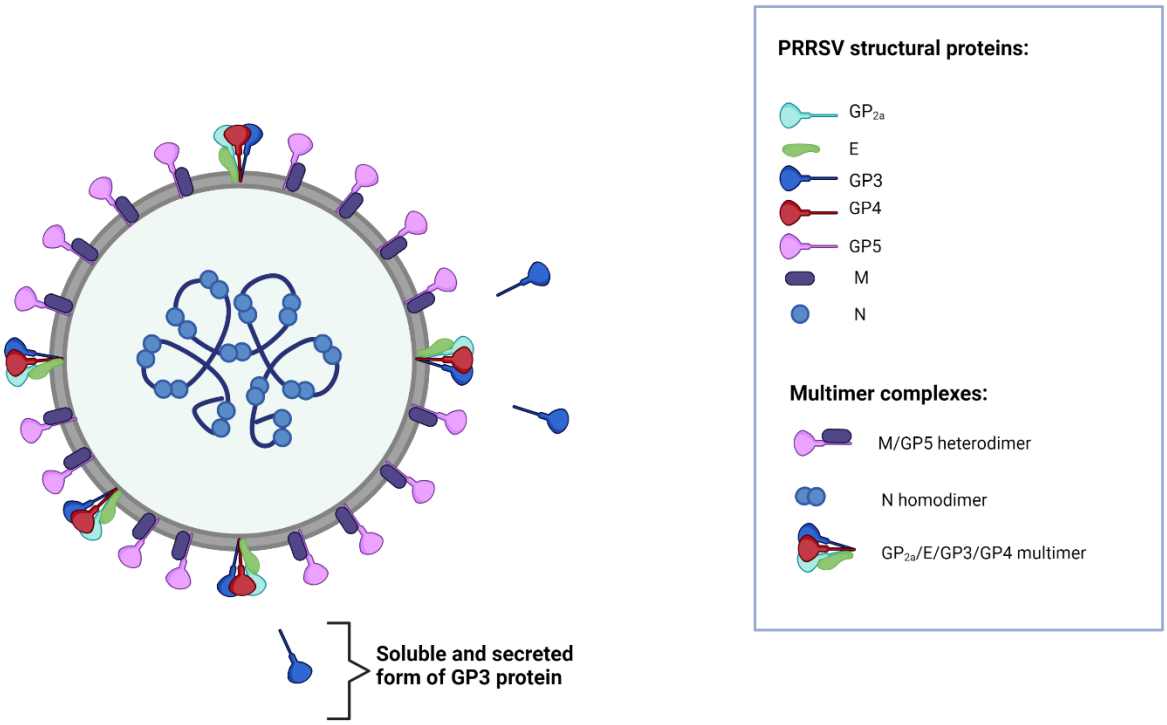

Figure 1. Schematic representation of the PRRSV particle. The locations of the structural proteins: GP2a, E, GP3, GP4, GP5, M and N (encoded by ORFs 2–7) are shown. The virion possesses a non-segmented single-stranded RNA genome which is polyadenylated at his 3' end, enclosed in a nucleocapsid protein (N), yielding a helicoidal capsid structure. The N protein is the sole component of the viral capsid and interacts with itself through covalent and non-covalent interactions (homodimer). The major envelope viral protein (GP5) forms a heterodimer structure with the membrane non-glycosylated protein (M) which dominates the virion surface. The minor structural proteins (GP2a, E, GP3 and GP4) are incorporated into virions as a multimeric complex. The minor structural viral proteins multimeric complex also interacts with the GP5-M heterodimer (not illustrated). Although GP3 is a structural viral protein, there is one report indicating that it is a non-structural and secreted viral protein (which suggests that this could be a strain-dependent phenomenon) [41].

Being an enveloped virus, PRRSV survivability outside of the host is affected by temperature, pH and exposure to detergents [18]. It is well documented that PRRSV can survive for extended intervals (>4 months) at temperatures ranging from -20 to -70°C when preserved in medium [20]. However, viability decreases with increasing temperature. Specifically, recovery of PRRSV has been reported for up to 20 min at 56°C, 24 h at 37°C, and 6 days at 21°C when incubated [20]. The PRRSV remains stable at pH ranging from 6.5 to 7.5. However, infectivity is reduced at pH $\geq$ 7.65 [44]. Detergents are effective at reducing infectivity of the virus, and lipid solvents such as chloroform and ether are particularly efficient at disrupting the viral envelope and inactivating replication [20].

2.5 Genome

PRRSV genome structure will not be discussed in depth. However, a brief analysis on the viral genome specific features will be presented. The PRRSV genomic RNA is a positive-stranded, 3 -polyadenylated molecule approximately 15 kb in length, which contains at least 11 known open reading frames (ORFs) [8, 42].The largest ORF is ORF1 which is located in the 5'-proximal three quarters of the polycistronic genome [8, 42]. It includes ORFs 1a and 1b. The ORFs 1a and 1b regions encode two large non-structural polyproteins, pp1a and pp1ab, which succeeding their synthesis are processed into at least 16 non-structural proteins (nsps) which are essential for the replication process [8, 42]. The 3'-distal end of the viral genome contains eight relatively small genes, and these genes have both 5' and 3'-terminal sequences overlapping with neighboring genes, apart from ORF4/ORF5 of type 2 PRRSV [8]. These genes encode four membrane-associated glycoproteins (GP2a, GP3, GP4, and GP5), three unglycosylated membrane proteins (E, ORF5a, and M), and a nucleocapsid protein (N) [8]. A schematic presentation of the PRRSV genome and structural organization is presented in Figure 2 including different sub-genomic RNAs formed during viral replication, which will not be covered, however, a more extensive review is provided by Kappes et al(2015) [42].

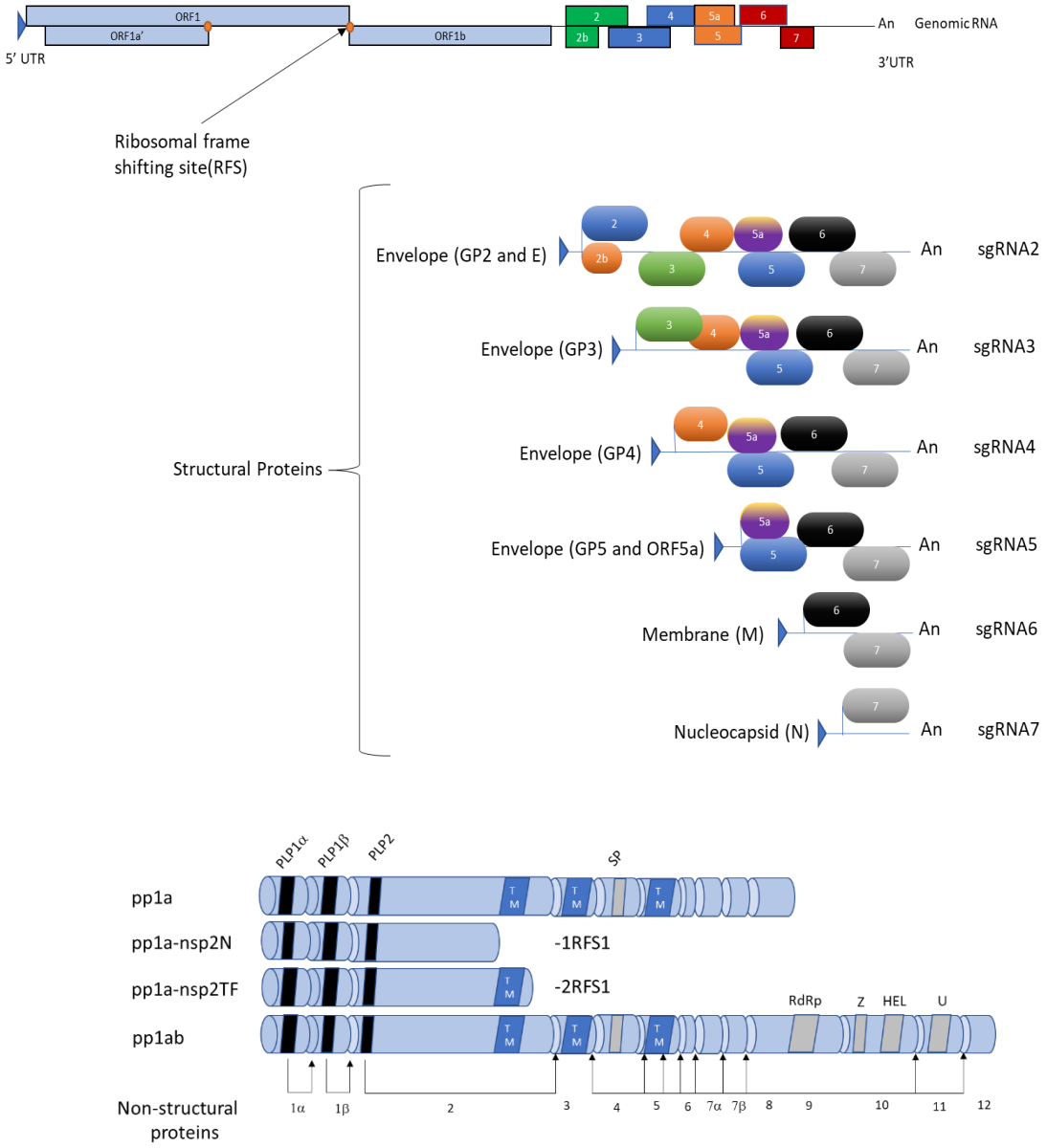

Figure 2. PRRSV genome, transcription, and translation. PRRSV replication progresses by a range of genetic and protein regulatory mechanisms. Expression of the first two-thirds of the 14.9-15.5 kb genome yields 4 known polyproteins (pp1a, pp1a-nsp2N, pp1a-nsp2TF, pp1ab) through two documented RFS. Polyproteins are co-translationally processed into at least 16 distinct nonstructural proteins (nsps) by four viral encoded proteases, PLP1a, PLP1b, PLP2, and SP. Recognized polymerase motifs in pp1ab are the RNA dependent RNA polymerase (RdRp), the zinc-finger domain (Z), the helical domain (HEL) and the nidovirus uridylate-specific endoribonuclease (U) domain. Canonical structural proteins are expressed exclusively through a set of subgenomic RNAs (sgRNA; 2-7) via a co-terminal discontinuous transcription strategy via a negative sense strand intermediate. Each subgenomic RNA are expressing only the ORF gene located at the 5' end location [42].

2.6 Structural proteins and non-structural proteins

Viruses depend on their host cell's resources to reproduce. They utilize the host cell's machinery to produce the viral proteins they require for replication [45, 46]. The majority of structural viral proteins are components of the capsid and the envelope of the virus whereas, non-structural counterparts are expressed in infected cells to promote the direct replication of the virus or indirectly by taking control of the cellular machinery and the immune response of the infected host [45].The roles of the various structural and non-structural proteins will be discussed briefly in this text, a more in depth review is provided by Music et al (2010) [41].

2.6.1 Structural proteins

The large number of envelope proteins is characteristic of *nidoviruses*, and all structural proteins were shown to be essential for infectivity [43, 47]. Arterivirus particles contain at least eight envelope proteins, an unusually large number among RNA viruses. These appear to divide into three groups: major structural components (major glycoprotein GP5 and membrane protein [M]), minor glycoproteins (GP2a, GP3, and GP4), and small hydrophobic proteins (E and the more recently discovered ORF5a protein) in addition to the nucleocapsid protein (N) [41, 43, 48]. Among the multitude of structural proteins of the PRRSV, the GP5 protein appears to be the most abundant on the envelope [41, 43]. The GP5 and M proteins are found in the form of dimers maintained by disulfide bonds [41]. These dimers are responsible for the assembly and budding of the virus and are important for the entry of the virus into the cell [41]. The unglycosylated N protein possesses 123 to 128 amino acids (aa) depending on the genotype of the strains (PRRSV-2 and PRRSV-1 respectively) [41], it is highly immunogenic and therefore, a suitable candidate for the surveillance of an infection; additionally, it is the sole component of the viral capsid and interacts with itself through covalent and non-covalent interactions. Furthermore it is able to localize in the nucleus/nucleolus and interact with cellular transcription factor [41].

The envelope protein (E) possesses molecular weight of 10 kDa and has been proven to be essential for the infectivity of the virus but not for particle assembly [41, 43]. This protein is associated with three other viral proteins (GP2a, GP3 and GP4) with which it forms a multimeric complex (Figure 1) [41, 43]. The GP2a, GP3 and GP4 proteins are encoded respectively by ORFs 2a, 3 and 4. They are composed of approximately 250 aa for GP2a, 260 aa for GP3 and 180 aa for GP4 [41].The GP2a contains 2 two highly conserved putative N-linked glycosylation sites; in addition to being immunogenic and antigenic[41]. GP3 is the most heavily glycosylated protein which is found in the viral envelope in PRRSV-1 strains or is secreted into the environment by cells infected with the PRRSV-2 strain [43]. This protein is highly antigenic, furthermore it seems to have a minor role in the neutralization of the virus [41]. Finally, the protein GP4 is involved in the interference of cellular mRNA synthesis [41, 43].

2.6.2 Non-Structural proteins

Non-structural proteins (nsps) are proteins which are essential for the viral cycle, these proteins are encoded by ORFs 1a and 1b and are consequently the first viral proteins to be translated; ergo allowing the viral replication cycle to begin [41, 43]. Nsp1 is composed of about 380aa, it is a multifunctional regulatory protein involved in transcription and virion biogenesis [41]. Nsp2 is the largest PRRSV replicative protein; it incorporates the major genetic differences between PRRSV-2 and PRRSV-1 strains, making it an ideal marker for monitoring genetic variation and for developing differential diagnostic tests [41, 43]. Nsps 9, 10 and 11 have been shown to have viral transcription and replication functions, with nsp9 being the RNA-dependent RNA polymerase (RdRp) and nucleoside-triphosphatase (NTPase), nsp10 being a helicase and finally nsp11 being involved with interferon (IFN) inhibition [41]. It is noteworthy to mention that Li et al. (2014) found that the nsp9 and nsp10 increase the virulence of the atypical HP-PRRSV that has emerged in China [49].

2.7 PRRSV host tropism factors

PRRSV is a virus known to possess a tropism towards cells of the monocytic lineage, specifically the porcine alveolar macrophages (PAM) [8, 50]. Among many different cell lines tested, only the African green monkey kidney cell line MA-104, and derivatives such as MARC-145 and SJPL, are fully permissive to PRRSV replication in vitro [8, 51]. The parameters limiting the entry of viruses into cells is the presence of membrane receptors [52]. Inhibition of an essential receptor results in inhibition of PRRSV [53]. These receptors were previously thought to be heparan sulfate, sialoadhesin (also called CD169) and the differentiation cluster 163 (CD163) [53]. However, more recent studies have shown that CD163 is the only essential receptor, and it acts post entry into the cells [54-56]. Figure 3 below demonstrates PRRSV entry mechanism into its target cell and the replication process.

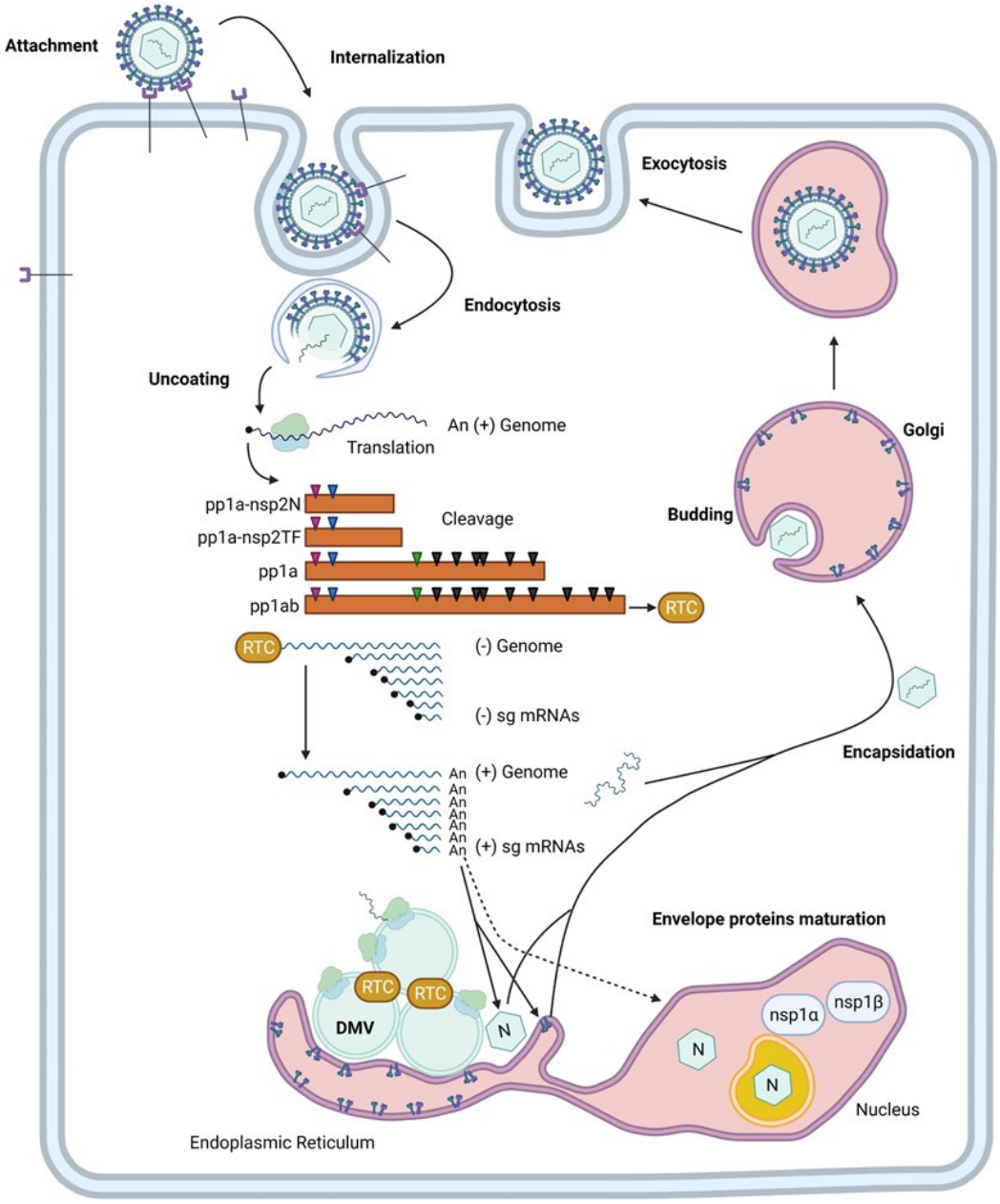

Figure 3. A demonstration of the virus entry mechanism and replication process of PRRSV. PRRSV enters host cells through standard clathrin-mediated endocytosis. The viral genome is released into the cytosol following endosome acidification and membrane fusion [8]. It is noteworthy to mention that a novel study has suggested PRRSV entry into the cell is through macropinocytic or phagocytic uptake pathways [56].Further investigations are required to fully understand the entry mechanism of PRRSV.

2.8 Immune response

Infection with PRRSV elicits poor innate and adaptive immune responses associated with immune modulation through dysregulation of NK cell function and IFNα production [57] and incomplete viral clearance in most of the pigs, depending on their age and immune status [58]. Nursery pigs suffer from PRRSV infection more than adult animals, owing to their poorly developed innate immune system as well as limited response to counter viral immune evasion strategies [59]. For more in-depth information on the innate and adaptive immune response against PRRSV refer to C.L. Loving et al 2015 and J.K. Lunney et al 2016 [8, 58].

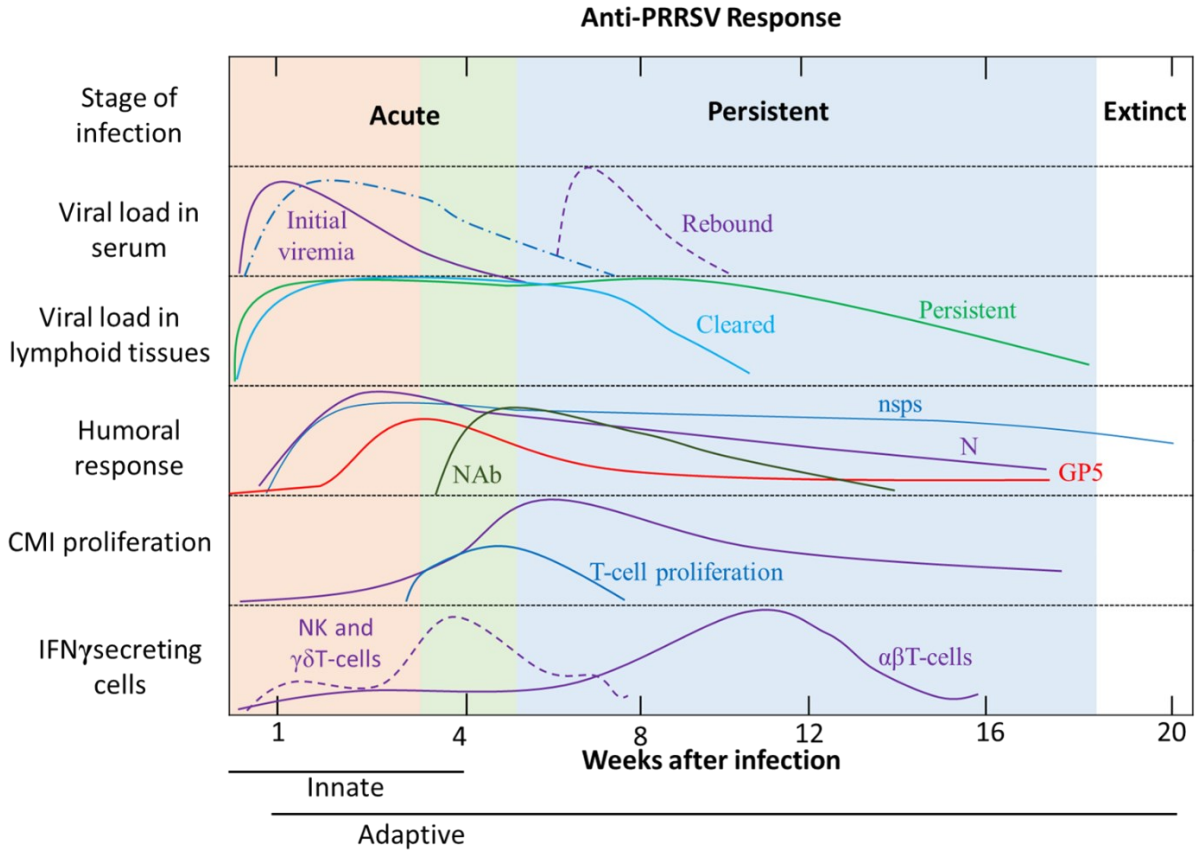

Figure 4. Immune response to porcine reproductive and respiratory syndrome virus (PRRSV) infection. Time points are approximate and could be changed depending on the virus isolate. Viral load in serum is indicated by a range of responses (solid purple for fast serum clearance and dashed blue for slower clearance, dashed purple for rebound virus). The timing of the humoral response is shown as neutralizing antibodies (NAb) and antibodies to PRRS viral proteins: N, GP5, and nonstructural proteins (nsps). Antibodies against nsps are predominantly to nsp1 (α/β), nsp2, and nsp7 (α/β); the other nsps induce low level or undetectable antibody responses. Cell-mediated immune (CMI) responses are weak early and peak later after PRRSV infection, with interferon-γ (IFNγ) secretion from natural killer (NK) and γδT cells early, followed later from αβ T cells [8].

2.9 Preventive measures

To date effective treatment for PRRSV has been found to be unsatisfactory. For this, various inactivated and attenuated vaccines have been marketed. Attenuated or inactivated vaccines are not very effective and generally only succeed in inducing a partial immune response [60]. Passive immunization has also been shown to be a way to protect pigs. Passive immunization consists of regular injections of porcine anti-PRRSV antibodies [61]. The identification of natural components capable of blocking or interfering with the replication of the PRRSV is a very promising avenue of research. In past years, studies have shown that molecules such as ouabain or valinomycin were able to inhibit virus replication in vitro [62]. Certain peptides have also been shown to be able to interfere with PRRSV and have an antiviral effect against it *in vitro* [63]. Another group has demonstrated anti-PRRSV activity of a component of the fungus *Cryptoporus volvatus* [64]. This compound appears to be active both *in vitro* and *in vivo* [64]. Studies in our group have also shown that *Actinobacillus pleuropneumoniae (App)* supernatant possesses an antiviral effect against PRRSV *in vitro* [12, 14]. If these unknown molecules prove to be as active *in vivo* as they are *in vitro*, it could introduce novel strategies for PRRSV control.

3. Bacterial and viral co-infections

Polymicrobial respiratory disease caused by viruses, bacteria and parasites are a major health concern in species bred under confined conditions in large groups. Often, multiple infectious agents are involved in the development of clinical signs, rendering the common reductionist approach of host-pathogen interactions by the study of a single infection unsuitable for the development of effective treatment models against the disease [10]. Co-infections have been described in both humans and animals. Moreover, bacterial and viral co-infections might be followed by secondary bacterial or viral infections, which in some cases are responsible for the pathology development and the observed clinical signs [10]. The following sections will focus on the PRRSV/*App* co-infection model.

3.1 *Actinobacillus pleuropneumoniae*

Actinobacillus pleuropneumoniae (App) is a small, Gram-negative, encapsulated rods bacterium with typical coccobacillary morphology [65]. The organism was first isolated in 1957 in Great Britain[66] and originally named *Haemophilus pleuropneumoniae* [67]. *App* was later assigned to the *Pasteurellaceae* family and *Actinobacillus* genus [65]. The main disease associated with this bacterium is porcine pleuropneumonia, a highly contagious respiratory disease, affecting especially young pigs [68, 69]. Acute disease, characterized by fibrino-haemorrhagic and necrotizing pleuropneumonia, is often fatal [70]. Asymptomatic carriers of the bacterium, either those having survived acute disease or those that were sub-clinically infected, may harbour *App* in nasal cavities, tonsillar crypts, and chronic lung lesions, thus becoming a source of infection for naïve subpopulations [71, 72].

3.1.1 Serology

In vitro, *App* is divided into two biotypes or biovars. Depending on their requirement for nicotinamide adenine dinucleotide (NAD) to grow, *App* strains can be further classified as biovar I (also called “typical”) that are NAD-dependent, or biovar II (or “atypical”) that are NAD-independent [65]. So far, 19 serovars of *App* are known, which differ in their capsular polysaccharide composition, with serovar 19 identified only recently [73]. Normally, serovars 1-12 and 15-16 are biovar 1, and serovars 13 and 14 are biovar 2 [65].

It has been shown that the virulence of *App* strains can be serovar or biovar-related, which is dependent, to some extent on, the respective production of Apx toxins [74-77]. Factors other than Apx toxins may also contribute to serovar-specific differences in virulence. However, other than capsule and lipopolysaccharides (LPS), which, by their nature contribute to differentiating serovars, little is known regarding the distribution of other various putative virulence factors among the different serovars of *App* [65]. A genomic comparison has indicated potential virulence-associated genes conserved among the more virulent serovars [78]; however, this study was based on genome sequences from single isolates, and not all serovars were represented.

Reported differences in virulence of certain isolates of the same serovar may be due, at least in part, to lack of production of one of the Apx toxins through deletion, point mutation or insertion of a transposon such as ISApl1. For example, serovar 2 strains from Europe are highly virulent, while North American isolates of the same serovars are almost non-virulent [65]. The low virulence North American biovar 1 serovar 2 isolates lack ApxIII, which is expressed by most European biovar 1 serovar 2 isolates [65].

3.1.2 Apx Toxins

Regarding virulence, major importance is to be given to the Apx toxins, with different degrees of cytotoxicity, haemolytic activity and distribution among serovars [79, 80](See Table 3).

Table 3. Haemolytic activity and cytotoxicity of various Apx toxins

Apx Toxin	Haemolytic Activity	Cytotoxicity	Serovars
ApxI	Strong	Strong	1,5a,5b,9,10,11,14 and 16
ApxII	Weak	Moderate	Present in all serovars except 10 and 14
ApxIII	None	Strong	2,3,4,6,8 and 15

A fourth RTX toxin, ApxIV, has not been characterized yet with regard to haemolytic or cytotoxic capacity [65]. It is noteworthy to mention that it is produced by all serovars *in vivo* and is therefore widely used for diagnostics [81].

3.2 PRRSV-*App in vitro* interaction

In a study done by Provost et.al in 2012 [51], a new permissive cell line to PRRSV, the SJPL, was identified. The SJPL cell growth was significantly slower than MARC-145 cell growth and was found to express the CD151 protein but not the CD163 and neither the sialoadhesin PRRSV receptors. However, SJPL cells were found to be permissive to PRRSV infection and replication even if the development of the cytopathic effect was delayed compared to PRRSV-infected

MARC-145 cells [51]. Following PRRSV replication, the amount of infectious viral particles produced in SJPL and MARC-145 infected cells was found to be similar. The SJPL cells allowed the replication of several PRRSV North American strains and were almost as efficient as MARC-145 cells for virus isolation. Interestingly, it was shown that PRRSV is 8 to 16 times more sensitive to IFNα antiviral effect in SJPL cells when compared to MARC-145 cells. PRRSV induced an increase in IFNβ mRNA and no up regulation of IFNα mRNA in both infected cell types. In addition, PRRSV induced an up regulation of IFNγ and TNF-α mRNAs only in infected MARC-145 cells [51].This provided an additional tool that could be used for the study of PRRSV pathogenesis mechanisms *in vitro* which is phenotypically different from MARC-145 cell line which is more commonly used [51].

In 2014 Levesque C. et al [12],explored the *in vitro* interactions between PRRSV, *App* and the host cells in the context of mixed infections or co-infections. To achieve their objective, they utilized three PRRSV permissive cell lines, namely, the MARC-145, SJPL and porcine alveolar macrophages (PAM). A pre-infection with PRRSV was performed at 0.5 multiplicity of infection (MOI) followed by an infection with *App* at 10 MOI. Bacterial adherence and cell death were compared. Results showed that PRRSV pre-infection did not affect bacterial adherence to the cells. PRRSV and *App* co-infection produced an additive cytotoxicity effect. However, a pre-infection of SJPL and PAM cells with *App* completely blocked PRRSV infection [12]. It was also revealed that incubation of SJPL and PAM cells with an *App* cell-free culture supernatant was sufficient to significantly block PRRSV infection. This antiviral activity was attributed to small molecular weight, heat-resistant *App* metabolites (<1 kDa) and not due to LPS [12]. The antiviral activity was also observed in SJPL cells infected with equine herpes virus type 1, swine influenza H1N1 and H3N2 but at a much lower extent compared to PRRSV. More importantly, the PRRSV antiviral activity of *App* was also seen with PAM, the cells targeted by the virus *in vivo* during infection in pigs. It was hypothesized that the antiviral activity might be due, at least in part, to the production of interferon γ [12].

3.3 Antiviral activity against PRRSV

In SJPL cells, co-infection with *AppΔapxICΔapxIIC*(mutant strain) and PRRSV showed an absence of PRRSV N viral protein detection by immunofluorescence assay (IFA) compared to control where SJPL cells were infected with PRRSV alone , suggesting an inhibition of PRRSV infection and/or replication [12]. MARC-145 cells were used to compare results obtained with SJPL cells since MARC-145 cells are the most common cells used during *in vitro* PRRSV studies [12]. Results were different between the two cell lines. In PRRSV infected MARC-145 cells, only a small reduction of cells expressing the PRRSV N protein was observed following a co-infection with *AppΔapxICΔapxIIC* [12]. SJPL cells proved to be qualitatively more responsive to the *App* antiviral effect than MARC-145 cells. Moreover, since SJPL cells were shown to be from monkey origin and not from swine as first described [82, 83], evaluation of the antiviral activity of *App* was tested in a porcine relevant cell model, the PAM cells. Co-infection with *AppΔapxICΔapxIIC* and PRRSV in PAM cells also presented total absence of PRRSV N protein detection, as in SJPL cells, suggesting that *AppΔapxICΔapxIIC* can also inhibit PRRSV in the virus's *in vivo* porcine target cells [12].

However, incubation with UV-inactivated *AppΔapxICΔapxIIC* bacteria after PRRSV infection allowed the detection of N proteins of PRRSV by IFA in all cell types showing that UV-inactivated bacteria were not able to block PRRSV infection. Interestingly, the bacteria-free culture supernatant of *AppΔapxICΔapxIIC* also effectively blocked PRRSV infection in SJPL and PAM cells. Whereas only a weak inhibition was observed in MARC-145 cells [12]. The active metabolites present in the culture supernatant were deemed not to be *App* LPS nor peptidoglycan fragments (assayed with NOD1 or NOD2 ligands). Dilutions of *AppΔapxICΔapxIIC* supernatant showed a dose-dependent effect on PRRSV's detection by IFA. A 1:2 dilution resulted in twice as much PRRSV N protein when observed with IFA [12].

3.3.1 *App* supernatant effect on SJPL cell cycles

Barbosa et al. 2015, hypothesized that the culture supernatant of *App* induced a specific SJPL cell response which has an antiviral activity against PRRSV [14].Their first objective was to

identify the mechanism behind the antiviral activity displayed. The second objective was to identify the molecules present in the *App* culture supernatant which are responsible for the antiviral activity against PRRSV [14].

An antibody microarray was used to identify cell pathways modulated by the *App* culture supernatant, and to observe modulations in cell cycle regulation pathways. To confirm these modulations, they performed a cell cycle analysis using flow cytometry [14].The microarray antibodies data suggested that *AppΔapxICΔapxIIC* culture supernatant modulates SJPL cell cycle, a decision to analyze SJPL and MARC-145 cell cycle after an 18h treatment with the *App* culture supernatant was made, using flow cytometry [14].

Following validation with cell cycle controls, SJPL cells were treated with the *App* culture supernatant and significant variations in SJPL cell cycle proportions were observed [14]. On average, the proportion of SJPL cells in G1-phase stayed the same as untreated cells (45.0 %). However, the proportion of SJPL cells in S-phase and in G2/M-phase significantly decreased to 21.1 % and increased to 33.9 %, respectively, indicating that *App* culture supernatant influenced SJPL cell cycles[14]. The ≤ 3kDa *App* culture supernatant ultrafiltrate which has been shown to possess the antiviral activity against PRRSV was also shown to modulate SJPL cell cycles[14]. The ≤ 3kDa *App* culture supernatant ultrafiltrate significantly increased the number of cells in G2/M-phase from 11.8 % to 22.1 % [14]. In order to determine whether the cell cycle arrests caused by the *App* supernatant were responsible for the antiviral activity, two known cell cycle inhibitors, SBE-13 and DIM, were tested to see if they can also block PRRSV infection. Interestingly, when infected SJPL cells were treated with DIM and SBE-13 there was an absence of PRRSV. This suggested a potential link between cell cycle arrest in G2/M-phase and antiviral activity against PRRSV in SJPL cells, which also highlighted the importance of cell cycles in PRRSV infection [14]. Contrarily, no modulation of the cell cycle was observed in MARC-145 cells treated with the *App* culture supernatant.

To identify the molecules which are present in the *App* supernatant that are responsible for the antiviral activity, mass spectrometry was used. The ≤ 3 kDa DMEM and ≤ 3 kDa *AppΔapxICΔapxIIC* culture supernatant ultrafiltrates were first fractionated to remove undesired inorganic molecules [14]. Supernatant was then analyzed in full scan positive ion mode by LC-

MS/MS and results are presented with a total ion current chromatogram (TIC). Both ≤ 3 kDa DMEM ultrafiltrate and ≤ 3 kDa *AppΔapxICΔapxIIC* culture supernatant ultrafiltrate were then compared and two unique peaks were observed in the ≤ 3 kDa *AppΔapxICΔapxIIC* culture supernatant ultrafiltrate [14]. Full scan spectra and extracted ion chromatograms showed the presence of two individual peaks at mass to charge (m/z) 515.2 and m/z of 663.6. The product ion spectra for these two peaks were acquired. At m/z 515.2, four ions were observed at m/z 161; 240; 329; 348, and six ions were observed for m/z 664 at m/z 495; 496; 551; 552; 607; and 608. However, due to the low-resolution instrument that was in use at the time, unequivocal identification of the molecules was not possible [14].

In the most recent study conducted by Reyes et al. 2018 [13], the way in which *App* culture supernatant inhibits PRRSV replication in its natural targeted host cells, i.e. PAM was analyzed. Several assays were conducted with PRRSV infected PAM, SJPL and MARC-145 cells that were treated with the *App* supernatant. RT-qPCR assays were used to determine the expression levels of type I and II IFN mRNAs, viral genomic (gRNA) and sub-genomic RNAs (sgRNAs). Proteomics, Western blot and immunofluorescence assays were conducted to determine the involvement of actin filaments in the *App* culture supernatant antiviral effect [13].

It was observed in this study that type I and II IFN mRNA expressions were not upregulated by the *App* culture supernatant [13]. Time courses of gRNA and sgRNA expression levels demonstrated that the *App* culture supernatant inhibits PRRSV infection before the first viral transcription cycle. Western blot experiments confirmed an increase in the expression of cofilin (actin cytoskeleton dynamic regulator) and immunofluorescence also demonstrated a significant decrease of actin filaments in *App* culture supernatant-treated PRRSV-infected PAM cells. *App* culture supernatant antiviral activity was also demonstrated against other PRRSV strains of genotypes I and II [13].

The conclusion of the study was that *App* culture supernatant antiviral effect against PRRSV takes place early during PRRSV infection. From the results obtained, it was hypothesized that *App* culture supernatant antiviral effect may take place via the activation of cofilin, which induces actin depolymerization and subsequently, probably affects PRRSV endocytosis. However, further experimentation was needed to fully validate this latest hypothesis and to

discover the active metabolites that are present in the *App* culture supernatant which are responsible for the antiviral effect [13]. It is note worthy to mention that many studies have been done with regards to the relationship between different viruses and their interaction with the actin cytoskeleton, one example of this is Epstein–Barr virus (EBV), analysis of EBV-transformed lymphocytes revealed substantial increases in the levels of actin and tubulin in these cells compared with levels in untransformed cells and in the sera of healthy individuals [84]. Surprisingly, actin and tubulin accumulated on the surface of EBV-transformed cells in large quantities [85].

4. Nucleosides

The term “nucleoside” was first used by Levene and Jacobs (1909) [86]. It is of great importance to understand the differences between nucleotides and nucleosides, they have different properties and therefore may have different pharmacokinetics (PK) and pharmacodynamics (PD). A single nucleotide is made up of three components: a nitrogen-containing base, a five-carbon sugar (pentose sugar), and at least one phosphate group. With all three combined, a nucleotide is also termed a “nucleoside phosphate” [87, 88]. In contrast, a nucleoside has only a nitrogenous base and a pentose sugar [87, 88].

4.1 Classification and metabolic functions

Nucleoside metabolites are classified based on their nitrogenous base and their pentose sugars. There are five major bases which are found in cells, and these five bases are the derivatives of purine and pyrimidine [88]. Adenine and guanine are the derivatives of purine and possess two rings Adenine has an ammonia group on its rings whereas guanine has a ketone group [87]. Cytosine, thymine and uracil are the derivatives of pyrimidines and possess one ring [87]. Thymine (found in DNA) and uracil (found in RNA) are similar in that they both have ketone groups, but thymine has an extra methyl group on its ring [87]. Based on the nitrogenous bases present, nucleoside derivatives maybe be grouped as the following: (i)Adenosine nucleotides: Adenosine triphosphate (ATP), ADP, AMP and Cyclic AMP (cAMP) (ii)Guanosine nucleotides:

GTP, GDP, GMP and cGMP (iii)Cytidine nucleotides: CTP, CDP, CMP (iv)Uridine nucleotides: UDP[87, 88]. Figure 5 presented below shows the different structures of various nitrogenous bases and their derivatives.

Both nucleosides and nucleotides play important roles in the replication and transcription of genetic information, and, as such, have been utilized for decades for chemotherapy, antiparasitic, antibacterial or antiviral therapeutics [86]. They are of great importance to living organisms, as they are the building blocks of nucleic acids (DNA and RNA), the substances that control all hereditary characteristics [87]. Ideally, a nucleoside/tide analogue would mimic the structure of a natural nucleoside enough to be recognized by cellular or viral enzymes and be incorporated into the DNA or RNA replication cycle, however, these analogues would possess one or more modifications that would then lead to the disruption and/or termination of replication [86]. Nucleosides/tides have a variety of roles in cellular metabolism, they are the energy currency in metabolic transactions and act as essential chemical links in the response of cells to hormones and other extracellular stimuli [87]. They are the structural components of an array of enzyme cofactors and metabolic intermediates such as coenzyme A (CoA) [88]. The structure of every protein, and ultimately of every biomolecule and cellular component, is a product of information programmed into the nucleoside/tide sequence of a cell's nucleic acids [87, 88].

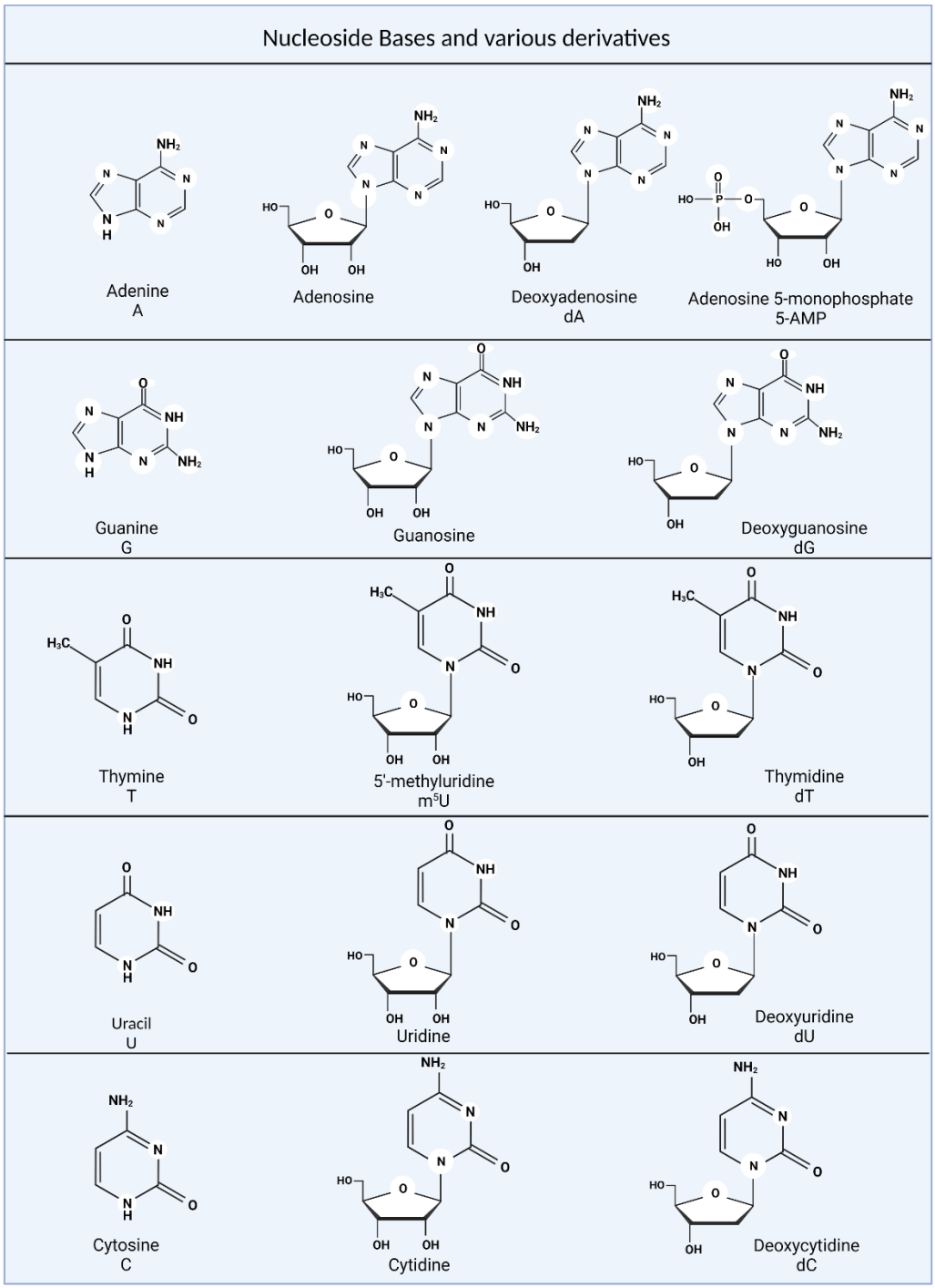

Figure 5. A schematic presentation demonstrating the structure of various nitrogenous bases and their derivatives.

4.2 Major classes of nucleoside analog drugs and prodrugs

Over the years, numerous modifications to the nucleoside/tide scaffold have been made, including alterations to the sugar, nucleobase, glycosidic bond, and phosphate group [86].These modifications range from adding a substituent or group to the heterocyclic base or sugar, replacing an atom in either moiety, by moving an atom to a different position, or a combination of these approaches [86]. More recently, researchers have employed the latter, utilizing a combination of many different types of modifications, which has led to the development of a wide array of potent nucleoside therapeutics, with complex structures [86]. There are 5 major modifications being utilized as of recent, for more detailed knowledge review Seley-Radtke et al. [86, 89]. In the section below the numbers 1',2',3',4' and 5' refer to the positions of the carbon atoms on the cyclic compounds.

4.2.1 1'-Sugar modifications

Some of the most promising 1'-substituted C-nucleosides pursued recently were the 1'-substituted 4-aza-7,9-dideazaadenosine C-nucleosides developed by Gilead [89]. An SAR (structure-activity relationship) study focused on various 1'- substituted analogues found that the 1'-cyano analogue displayed a broader spectrum of antiviral activity against viruses such as Hepatitis C virus (HCV), yellow fever virus (YFV), dengue-2 virus (DENV-2), influenza A, parainfluenza 3, Ebola virus (EBOV) and severe acute respiratory syndrome coronavirus (SARS-CoV), with the best antiviral activity against EBOV in Human lung microvascular endothelial cells (HMVEC) cells (EC_{50} = 0.78 μM) [86, 89].

4.2.2 2'-Modifications

Numerous 2' modified nucleoside analogues have been developed, some of the most promising have been the 2'-methyl analogues, particularly those that have exhibited activity against HCV [90, 91]. Of these, 2'-methyl adenosine, 2'-methyl guanosine, and 2'- methyl cytidine (NM107) were initially pursued and all displayed micromolar levels of activity against HCV in whole-cell replicon assays [90, 91]. The adenosine analogue proved to be the most potent, with an EC_{50} of

0.26 μM compared to 3.5 μM for the guanosine analogue and 1.23 μM for the cytidine analogue [92-94]. Interestingly, none of these compounds demonstrated any cytotoxicity *in vitro* [91-94]. Unfortunately, they displayed low bioavailability as well as a high rate of deamination of the nucleobase in the 2'-methyl adenosine analogues and increased glycosidic bond cleavage by purine nucleoside pyrophosphorylase [93, 94]. The guanosine analogue also exhibited low bioavailability due to insufficient phosphorylation and decreased cellular uptake [93, 94]. While these initial studies were disappointing, they provided researchers with a starting point for developing the next generation of HCV nucleoside therapeutics.

4.2.3 3'-Modifications

Due to the initial success with the 2' modified nucleoside analogues, scientists also explored modifications at the 3' carbon. Some of the first 3' modified nucleosides include 3'- methyl analogues such as 3'-C-methyluridine and 3'-C-methylcytidine [89]. From these initial SAR studies, it was found that 3'-C-methyladenosine served as a potent anticancer agent against numerous human leukemia and carcinoma cell lines, with IC_{50} values of ~18 μM [89, 95]. Further analysis found that shifting the methyl from the 3' position of 3'-C-methyladenosine to another position on the sugar ring was associated with a decrease in activity, thus highlighting the importance of this moiety [89]. Similarly, this study found that the adenosine nucleobase was the most active analogue against human myelogenous leukemia K562 cells and human colon carcinoma HT-29 and CaCo-2 cell lines, with no antiproliferative activity found with the other nucleobases [89].To further test the ability of these 3'-C-methyl analogues as potential therapeutics, the Osolodkin group studied 3'-C-methyluridine and cytidine against Tickborne encephalitis virus, however, none of these analogues demonstrated potent antiviral activity [96].

4.2.4 4'-Modifications

Until the discovery of naturally occurring 4'-modified nucleoside analogues in 1956, modifications to the 4' position of the furanose ring was rather uncommon in drug design,

mainly due to the synthetic challenges [86]. As more facile synthetic routes were developed, more researchers began to pursue these interesting analogues. Researchers soon noted that modifications to the 4′ position of the furanose ring changed the sugar pucker from a C2′-exo/C3′-endo "north" conformation, as is common in natural RNA nucleosides [97], to a C2′-endo/C3′-exo "south" conformation [98]. This affects recognition by different enzymes, thus can have a significant impact on their biological activity [86].

4.2.5 5′-Modifications

While modifications to various positions of the furanose ring are very common, the importance of the 5′-hydroxyl group in nucleotide incorporation for both DNA and RNA synthesis initially caused researchers to avoid modifications at the 5′-position [86, 89]. In some instances however, as seen with the 5′-deoxy, 5′-nor, and truncated carbocyclic nucleosides related to Aristeromycin and Neplanocin developed by Schneller, Seley, Borchardt, and others, removal or replacement of the 5′-methylene group and/or 5′-hydroxyl group proved beneficial since these analogues could no longer be phosphorylated, thus the toxicity observed with the parent analogues Aristeromycin and Neplanocin did not occur with the truncated analogues [89]. Other researchers have also utilized these approaches to their advantage in order to decrease overall toxicity of various nucleoside analogues.

4.3 Mechanism of action

With the rise in use of nucleoside/tide analog drugs due to their displayed broad spectrum antiviral activity [99-101], came the need for increased efficacy of the drugs. One such example of this statement is the 1′-cyano analogue created by Gilead, in order to increase the delivery of this analogue they employed the McGuigan ProTide (PROdrug nucleoTIDE) approach [102-104]. The ProTide approach has proven extremely valuable for delivery of nucleotide analogues, as well as to overcome the rate-limiting first phosphorylation step (Figure 6). During DNA/RNA replication, nucleosides (and nucleoside analogues) are phosphorylated by various host cell or viral kinases into their triphosphate form, which are then recognized by DNA polymerases, RNA

polymerases, or reverse transcriptase and incorporated into the growing chain [105, 106]. Since the triphosphate cannot be administered directly due to the highly charged nature of the phosphate groups, the prodrug helps deliver the nucleotide into the cell. A second limitation associated with nucleoside drugs is that the first phosphorylation step is often highly specific and rate-limiting, thus the nucleoside analogue is often not recognized and appears inactive [103, 104, 107]. To overcome this obstacle, McGuigan et al. created ProTides that would efficiently deliver the monophosphate nucleoside analogue into the target cell, bypassing the rate-limiting first phosphorylation step [103, 104, 107, 108]. These ProTides utilize a unique structure, with three "tunable" positions - the aryl, the amino acid, and the ester groups [103, 104, 107, 108].The aryl group and the amino acid ester mask the negative charges on the monophosphate, allowing the ProTide to efficiently cross the cell membrane [104, 107, 108]. Following metabolism by various host enzymes, the monophosphate nucleotide analogue is successfully delivered and is subsequently phosphorylated into the active triphosphate [107, 108]. Using the McGuigan ProTide approach with the 1'-cyano compound produced GS-5734 (Remdesivir), which increased the overall anti-EBOV activity (EC_{50} = 0.06 μM compared to 0.78 μM for the parent). In addition, this also increased the spectrum of the antiviral activity to include viruses that the parent nucleoside was not active against, including West Nile virus (WNV), Lassa fever virus, and Middle East respiratory syndrome coronavirus (MERS-CoV) [109-111]. Further studies found that GS-5734 was an effective post-exposure therapeutic in EBOV-infected rhesus monkeys at 10 mg/kg [108, 111].

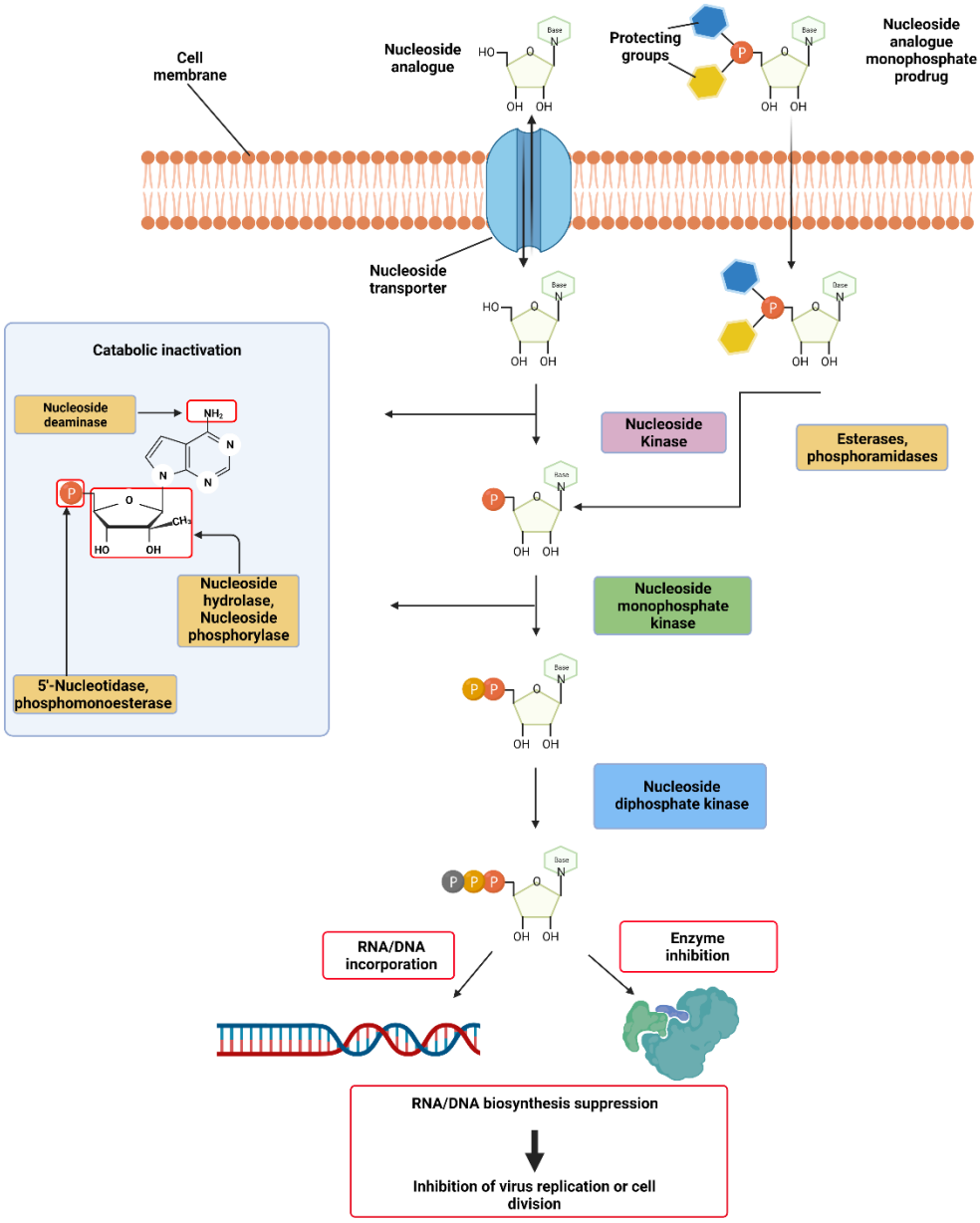

Figure 6. Intracellular uptake and metabolism of nucleoside analogs and nucleoside analog prodrugs. Nucleoside analogs enter cells through specific plasma membrane nucleoside transporters. Inside the cell, the compounds are phosphorylated by cellular nucleoside kinases resulting in formation of nucleoside mono-, di-, and triphosphates. The first kinase phosphorylation is the rate-limiting step of the triphosphate conversion, which can be overcome by the monophosphate prodrug approach based on the introduction of a phosphorylated group into the 5' nucleoside position. The phosphorylated group includes protecting moieties to increase hydrophobicity and facilitate the cellular uptake of the prodrug. Monophosphate prodrugs enter cells independently of membrane transporters and the protecting groups are removed by intracellular esterases or phosphoramidases after cell penetration. The triphosphates of nucleoside species represent the active forms of nucleoside analogs that act by inhibiting cellular or viral enzymes, such as DNA/RNA polymerases. During DNA/RNA replication, nucleoside analogs are incorporated into nascent DNA or RNA chains resulting in termination of nucleic acid synthesis or in accumulation of mutations in viral genomes to suppress viral replication due to error catastrophe [112].

5. Hypothesis and objectives

The problems associated with PRRSV and *App* are numerous, these two pathogens are among the pathogens affiliated with porcine respiratory disease complex and they cause substantial economic losses in pig producing countries worldwide. They are prevalent to this day, with PRRSV being one of the most important pathogens in the pork industry.

Based on previous conducted studies, we know that SJPL cells are permissive to several viruses such as human, avian, equine and porcine influenza viruses [83]. In addition to these viruses, previous work in our group has shown that it is permissive to and promotes viral replication of PRRSV as well [51]. SJPL was previously considered a porcine cell line hence the name: Saint-Jude porcine lung, but was later found to be mistakenly classified as porcine cells and were genetically identified discovered to be of monkey origins [82].

Knowledge obtained from previous research projects have been the basis of our current study [12-14, 51]. This led us to our main hypothesis which is: the culture supernatant of *App* contains specific unidentified primary and secondary metabolites which induce an antiviral activity against PRRSV in SJPL cells *in vitro*. The objectives of this project would be (i)to generate an active *App* supernatant, (ii)characterize and identify the unknown metabolites using high resolution mass spectrometry, and (iii)to evaluate the antiviral activity of the purified compounds following identification. This project is part of a global effort in developing new therapeutic and/or prophylactic approaches to combat infections caused by PRRSV.

ARTICLE

Untargeted and targeted metabolomics reveal that adenosine nucleotides released in *Actinobacillus pleuropneumoniae* supernatant inhibit porcine reproductive and respiratory syndrome virus replication

Abdulrahman Fuad Salmin[1,3], Marie-Jeanne Pesant[1], Yaima Burgher[1], Chantale Provost[1,2], Josée Labrie[4], Mario Jacques[4], Carl A. Gagnon[1,2], Francis Beaudry[1,3,5,*]

1- Centre de recherche en infectiologie porcine et avicole (CRIPA), Faculté de médecine vétérinaire, Université de Montréal

2- Laboratoire de diagnostic moléculaire, Service de diagnostic, Faculté de médecine vétérinaire, Université de Montréal

3- Groupe de recherche en pharmacologie animale du Québec (GREPAQ), Département de biomédecine vétérinaire Faculté de médecine vétérinaire, Université de Montréal

4- Groupe de recherche sur les maladies infectieuses en production animale (GREMIP), Faculté de médecine vétérinaire, Université de Montréal

5- Centre de recherche sur le cerveau et l'apprentissage (CIRCA), Université de Montréal, Montréal, QC, Canada

*Corresponding author:

Francis Beaudry, Ph.D.
Professor
Département de Biomédecine Vétérinaire
Faculté de Médecine Vétérinaire
Université de Montréal
3200 Sicotte
Saint-Hyacinthe, QC
Canada J2S 2M2

Email: francis.beaudry@umontreal.ca

Keywords: Porcine reproductive and respiratory syndrome virus (PRRSV), *Actinobacillus pleuropneumoniae (App)*, St. Jude Porcine Lung Epithelial Cell Line (SJPL), Antiviral, High-performance liquid chromatography, Mass spectrometry, Metabolomics, Adenosine nucleosides

Abstract

Porcine reproductive and respiratory syndrome virus (PRRSV) is one of the most devastating viruses in the swine industry and causes major economic losses. To date, there has not been an effective antiviral treatment for the disease. We have shown in previous studies that culture supernatant of *Actinobacillus pleuropneumoniae (App)*, the causative agent of porcine pleuropneumonia, possesses antiviral activity *in vitro* against PRRSV, and we have clearly established that the antiviral activity was mediated by small molecular weight (i.e., < 1 kDa), heat resistant metabolites present in the *App* supernatant ultrafiltrates. However, the identity of those metabolites remains unknown. The objective of the current study was to identify the active metabolites using untargeted and targeted mass spectrometry-based metabolomics and test their respective antiviral activity against PRRSV in the Jude Porcine Lung Epithelial Cell Line (SJPL). The results presented reveal very significant antiviral activity of *App* supernatant ultrafiltrates against PRRSV in SJPL cells. Consequently, we identified and quantified several adenosine nucleotide metabolites present in *App* supernatant ultrafiltrates using mass spectrometry-based metabolomics, and the concentrations detected were very high. SJPL cells infected with PRRSV and treated with 2'-adenosine monophosphate (2-AMP), 3'-adenosine monophosphate (3-AMP) or 5'-adenosine monophosphate (5-AMP) significantly reduced PRRSV infection. Interestingly, many antiviral drugs or prodrugs are adenosine analogs, and the mechanism of action was previously elucidated. Currently marketed nucleoside analog drugs could potentially be used to treat PRRSV infection.

1. Introduction

Porcine reproductive and respiratory syndrome (PRRS) is a worldwide endemic disease causing substantial economic losses in pig-producing countries. In sows, PRRS is characterized by reproductive failure, late-term abortions, increased numbers of stillborn fetuses, and/or premature and weak piglets [1–6]. During PRRS disease, increased morbidity and mortality in growing and finishing pigs as a result of severe respiratory disease and poor growth performance are frequently observed [7–8]. The infectious agent porcine reproductive and respiratory syndrome virus (PRRSV) is related to the Arteriviridae family of the Nidovirales order. PRRSV is an enveloped single-stranded positive-sense RNA virus comprising approximately 15 kb that encodes a minimum of 11 open reading frames (ORFs) [9]. Similar to several other RNA viruses, PRRSV genome heterogeneity denotes the main impediment to develop effective prevention and control of the disease using vaccination [10].

Actinobacillus pleuropneumoniae (*App*) is the causative agent of porcine pleuropneumonia, an important disease in the swine industry worldwide. In recent years, we have developed *in vitro* models to study host-pathogen interactions using an immortalized epithelial cell line, namely, St. Jude Porcine Lung (SJPL) cell line [11]. We have specifically used this model to study coinfections by *App* and porcine viral pathogens. These investigations were achieved since coinfections are likely more common than reported in the field and since a primary infection with a viral or bacterial pathogen may enhance the infectious potential of a secondary pathogen [15–17]. Interestingly, we unexpectedly observed that *App* culture supernatants have strong antiviral activity against porcine reproductive and respiratory syndrome virus (PRRSV) during *App*-PRRSV coinfections of SJPL cells [12]. Conversely, we recently published another study

confirming *the antiviral effect of App* culture supernatant [13]. *App* antiviral activity against PRRSV was also observed in porcine alveolar macrophages, the primary target cells of PRRSV during porcine infection [13]. As we reported, *App* inhibits PRRSV by inducing cell cycle arrest in the G2/M phase of SJPL cells [14]. Additionally, we unveiled that small molecular weight, heat-resistant metabolites present in *App* supernatant ultrafiltrates (< 1 kDa) and not LPS (extracted whole molecules) or peptidoglycan fragments (i.e., NOD1 and NOD2 ligands) are responsible for *App* antiviral activity [12]. Unfortunately, initial experiments using a low-resolution mass spectrometer (MS) instrument were unsuccessful for identifying potential candidates with strong confidence [14]. Therefore, the aim of the current study was to identify potential low molecular weight molecules using high resolution accurate mass (HRAM) mass spectrometry (MS) using untargeted and targeted workflows combined with specific bioinformatic workflows using curated databases (e.g., mzCloud, ChemSpider) and to examine the antiviral activity of these identified molecules.

2. Materials and Methods

2.1 Chemicals and reagents

All chemicals and reagents were obtained from Fisher Scientific (Fair Lawn, NJ, USA) or Millipore Sigma (St. Louis, MO, USA). 2'-Adenosine monophosphate (2-AMP), 3'-adenosine monophosphate (3-AMP), 5'-adenosine monophosphate (5-AMP), 2,3-cyclic adenosine monophosphate (2,3-cAMP) and 3,5-cyclic adenosine monophosphate (3,5-cAMP) standards were purchased from Millipore Sigma.

2.2 Bacterial and viral strains

Actinobacillus pleuropneumoniae nonhemolytic and noncytotoxic MBHPP147 was generously provided by Ruud P.A.M. Segers (MSD Animal Health, Boxmeer, The Netherlands). This strain is a mutant of the serotype 1 reference strain S4074 producing nonactive ApxI and ApxII toxins (App*ΔapxICΔapxIIC*) [19]. Bacteria were grown at 37 °C in brain heart infusion broth (BHI; Oxoid Ltd., Basingstoke, Hampshire, England) or in BHI agar Oxoid Ltd.) supplemented with 5 μg/mL or 15 μg/mL β-nicotinamide adenine dinucleotide (β-NAD; Sigma Aldrich, St Louis, MO, USA), respectively. The PRRSV North American reference strain IAFKlop was used in this study. This strain is a genotype II strain [20, 21].

2.3 Bacterial culture supernatant

Actinobacillus pleuropneumoniae culture supernatant was prepared as described by Lévesque and collaborators [12]. Briefly, an overnight culture of App*ΔapxICΔapxIIC* was diluted in fresh BHI broth, grown to an OD600 of 0.6 and diluted in DMEM supplemented with 10% FBS, 2 mM L-glutamine, 1 mM sodium pyruvate, and 1% NEAA to 1×10^6 CFU/mL. The culture was then incubated overnight at 37 °C. Bacterial cells were centrifuged at 4,000 *g* for 20 min, and the

supernatant was harvested and filtered using a Millipore Membrane 0.22 µm filter (Millipore Sigma). Filtered App*ΔapxICΔapxIIC* supernatant was ultrafiltrated using a 3-kDa membrane (Millipore Sigma). The App*ΔapxICΔapxIIC* supernatant ultrafiltrates were stored at −20 °C prior to use. Likewise, supplemented DMEM medium was ultrafiltrated through a 3-kDa membrane and used as a negative control.

2.4 PRRSV cells infection and detection

The protocol for cell infection was derived from Lévesque *et al*. 2014 [12]. Briefly, SJPL cells were infected with a 0.5 MOI of PRRSV and incubated in DMEM without serum or other additives for 4 hours. Then, the cells were washed with PBS to remove all nonattached viral particles. Fresh medium was added. One milliliter of App*ΔapxICΔapxIIC* supernatant ultrafiltrate or DMEM was added to each treated well 4 hours after PRRSV infection, and plates were incubated for 48 hours. The detection of PRRSV in SJPL cells was performed using a modified immunofluorescence assay (IF) protocol detecting PRRSV antigens [12–14]. Briefly, following infection and/or treatment, cells were washed and then fixed for 15 min at room temperature with a 50% (v/v) methanol and 50% (v/v) acetone solution. Cells were washed three times using phosphate-buffered saline without KCl (PBS): 0.1 M NaCl, 4 mM Na_2HPO_4, and 1.5 mM KH_2PO_4 and then incubated for 90 min at 37 °C with rabbit monospecific antisera (anti-PRRSV N protein) [21] diluted 1:150 in PBS. SJPL cells were washed three times with PBS and incubated at 37 °C for 60 min with FITC-conjugated anti-rabbit antiserum (Life Technologies) diluted 1:75 in PBS. Finally, SJPL cells were washed three times with PBS and visualized using a Leica DMI 4000 inverted widefield fluorescence microscope (Leica Microsystems Inc., Richmond Hill, Canada). Pictures were acquired using a DFC 490 digital camera (Leica Microsystems Inc.) and images were analyzed using Leica Application Suite Software, version

2.4.0 (Leica Microsystems Inc.) and ImageJ from the Laboratory for Optical and Computational Instrumentation (LOCI, University of Wisconsin) [22].

2.5 Mass spectrometry analysis

2.5.1 Sample Preparation

App*ΔapxICΔapxIIC* culture supernatant ultrafiltrates were diluted 1/5 (v/v) with ultrapure water and centrifuged at 12,000 g for 10 minutes. Two hundred microliters of sample was transferred into injection vials for analysis.

2.5.2 Untargeted metabolomic analysis

The UHPLC system was a Thermo Scientific Vanquish FLEX UHPLC system (San Jose, CA, USA). Chromatography was performed using gradient elution along with a GL Sciences Capillary EX column ODS-3 150 × 0.7 mm, with a particle size of 5 µm (Tokyo, Japan). The initial mobile phase conditions consisted of acetonitrile and water (both fortified with 0.1% formic acid) at a ratio of 2:98. From 0 to 2 min, the ratio was maintained at 5:95. From 2 to 92 min, a linear gradient was applied up to a ratio of 95:5 and maintained for 5 min. The mobile phase composition ratio was reverted under the initial conditions, and the column was allowed to re-equilibrate for 25 min. The flow rate was fixed at 50 µL/min, and 2 µL of sample was injected. A Thermo Scientific Q Exactive Plus Orbitrap Mass Spectrometer (San Jose, CA, USA) was interfaced with the UHPLC system using a pneumatic-assisted heated electrospray ion source. Nitrogen was used for sheath and auxiliary gases, and they were set at 10 and 5 arbitrary units. Auxiliary gas was heated to 200 °C. The heated ESI probe was set to 4000 V, and the ion transfer tube temperature was set to 300 °C. MS detection was performed in positive ion mode and operating in TOP-6 Data Dependent Acquisition (DDA) mode. A DDA cycle entailed one MS^1

survey scan (m/z 75–1000) acquired at 70,000 resolution (FWHM) and precursor ions meeting user-defined criteria for the charge state (i.e., z = 1 or 2), monoisotopic precursor intensity (dynamic acquisition of MS^2-based TOP-6 most intense ions with a minimum $5x10^4$ intensity threshold). Precursor ions were isolated using the quadrupole (1.5 Da isolation width), activated by HCD (stepwise 25, 30, 35 NCE) and fragment ions were detected in the Orbitrap at 17,500 resolution (FWHM). MS^1 and MS^2 data were further analyzed using Compound Discoverer 3.1 (Thermo Scientific, San Jose, CA, USA) to identify metabolite release in the App*ΔapxICΔapxIIC* culture supernatant. Chromatograms were aligned, and a list of potential metabolites was generated depending on the HRAM MS^1 and MS^2 measurements using mzVault, mzCloud and ChemSpider with the following parameters: within ± 5 ppm of mass error; retention time tolerance of ± 0.2 min; ion ratio tolerance within ± 30%; and isotopic pattern matching >80% of the precursor and the characteristic product ions. MS^2 spectra were compared specifically using a fully curated and annotated mass-spectral fragmentation library of mzCloud to confirm the identity of the detected metabolites or common substructural information to aid in secondary metabolite identification.

2.5.3 Targeted LC-SRM/MS analysis

The HPLC–MS/MS system included a Thermo Accela autosampler, a Thermo Accela pump and a Thermo LTQ-XL Linear Ion Trap Mass Spectrometer (San Jose, CA, USA). Chromatography was achieved using a gradient mobile phase along with a Thermo Aquasil C18 100 × 2.1 mm column with a particle size of 3 µm. The initial mobile phase conditions consisted of acetonitrile and water (both fortified with 0.1% formic acid) at a ratio of 2:98. From 0 to 1 min, the ratio was maintained at 2:98. From 1 to 12 min, a linear gradient was applied up to a ratio of 95:5 and maintained for 3 min. The mobile phase composition ratio was reverted under the initial conditions, and the column was allowed to re-equilibrate for 8 min for a total run time of 23 min.

The flow rate was fixed at 200 µL/min, and 2 µL of sample was injected. The mass spectrometer was coupled with the HPLC system using a pneumatically assisted electrospray ion source (ESI). The sheath gas was set to 35 units, and the ESI electrode was set to 4000 V in positive mode. The capillary temperature was set at 300 °C, and the ion transfer tube voltage was 45 V. All scan events were acquired with a 100 ms maximum injection time. An activation q = 0.25 and activation time of 30 ms were used for all targeted peptides. The mass spectrometer operated for quantitative analyses in SRM mode, and the mass transitions used were 348 → 136 and 330 → 136 for AMP- and cAMP-targeted nucleosides, respectively. Calibration standards were prepared in DMEM by spiking reference solutions to obtain an analytical range from 0.01 – 1.0 mM. The linearity of the method was determined by analysis of standard plots associated with a seven-point standard calibration curve. Semiquantitative analysis was performed using the peak area, and the concentrations observed in App*ΔapxICΔapxIIC* culture supernatant ultrafiltrates were interpolated from the standard curve.

3. Results and Discussion

3.1 Determination of *App* antiviral activity against PRRSV

SJPL is a PRRSV permissive cell line specifically used to test App*ΔapxICΔapxIIC* antiviral activity, as shown in previous manuscripts [12–15]. Treatment with App*ΔapxICΔapxIIC* culture supernatant ultrafiltrates (i.e., < 3 kDa) was performed after infection with PRRSV in SJPL cells. PRRSV antigen detection in SJPL shown in Figure 1A reveals that App*ΔapxICΔapxIIC* culture supernatant produces an antiviral effect against PRRSV. As revealed in Figure 1B, these results were confirmed based on the fluorescence intensity computation performed with ImageJ software. Unequivocally, these results and previous results [12–15] strongly suggest that low

molecular weight metabolites were potentially responsible for the antiviral effect observed. Therefore, we wanted to expand our investigations using mass spectrometry-based metabolomic analytical strategies to identify and quantify these molecules and potentially discover new pharmacological strategies for the treatment of PRRSV infections.

3.2 Untargeted metabolomics

To identify the molecules responsible for the App*ΔapxICΔapxIIC* culture supernatant ultrafiltrate antiviral effect, we first used an untargeted metabolomic strategy using a hybrid quadrupole-Orbitrap HPLC–MS system and a data-dependent acquisition (DDA) mode. Untargeted metabolomics is challenging because it aims to identify and quantify hundreds to thousands of different compounds with various chemical properties and structures with limited prior knowledge of the metabolites. It is, therefore, advantageous to use a mass spectrometer system that provides accurate mass information for confident confirmation and structural elucidation. Differential bioinformatic analyses were performed using Thermo Scientific Compound Discovered (ver 3.1) performing background subtraction, component detection, peak alignment, and differential analysis. Identifications were based on MS^1 and MS^2 mass spectral database matching (i.e., mzCloud and ChemSpider). An example is shown in Figure 2A. The untargeted DDA TOP-6 analysis of molecules present in App*ΔapxICΔapxIIC* culture supernatant ultrafiltrates reveals the presence of several nucleoside metabolites. Interestingly, in the TOP-5 most abundant (i.e., based on $\log_2$ fold-change), we found 3'-adenylic acid (3-AMP). As revealed in Figure 2B, extracted ion chromatograms (m/z 348.07036 ± 5 ppm) comparing the control sample (DMEM) and the App*ΔapxICΔapxIIC* culture supernatant ultrafiltrates showed an absence of 3-AMP in the control but very high abundance in the App*ΔapxICΔapxIIC* culture supernatant ultrafiltrates. Furthermore, the MS^2 spectra shown in Figure 2C comparing the

observed spectrum and curated reference spectrum extracted from mzCloud strongly support the identification of 3-AMP. Additionally, as we have pointed out in Figure 2A, other adenosine nucleoside metabolites (i.e., 2-AMP, 5-AMP, 2,3-cAMP and 3,5-cAMP) and other nucleosides were detected at high abundance. These results were unexpected but highly interesting since a wide variety of adenosine nucleoside analogs and prodrugs are currently available and exhibit antiviral activity against several RNA viruses [23, 24]. Moreover, it is important to note that nucleoside analogs constitute the main class of small molecule-based antivirals available on the market or under investigation. Database search and library annotations have limitations, still posing an important barrier to untargeted MS-based analyses for the identification of molecules. Therefore, we wanted to confirm the presence of these metabolites in the App*ΔapxICΔapxIIC* culture supernatant ultrafiltrates. As shown in Figure 3, we analyzed selected adenosine nucleoside reference standards using high-resolution HRAM-MS to collect MS^1 and MS^2 spectra. The MS^1 and MS^2 spectra collected were coherent with reference spectra extracted from mzCloud but did not allow us to distinguish adenosine monophosphate metabolites (2-AMP, 3-AMP and 5-AMP) or cyclic adenosine monophosphate metabolites (2,3-cAMP and 3,5-cAMP). The mass accuracy observed was within ± 5 ppm at the MS^1 and MS^2 levels. The MS^2 ions observed are coherent with the proposed MS^2 fragmentation scheme outline in Figure 4. As shown, MS^1 or MS^2 spectra are insufficient to differentiate adenosine monophosphate or cyclic adenosine monophosphate metabolites. Reanalysis of App*ΔapxICΔapxIIC* culture supernatant ultrafiltrates in targeted mode (i.e., full scan and targeted MS^2) was performed and confirmed the presence of adenosine monophosphate and cyclic adenosine monophosphate metabolites. As unveil in Figure 5, the MS^2 spectra of the most abundant peaks observed at m/z 348 and m/z 330 were coherent with the spectra collected from the reference material under identical conditions.

3.3 Targeted metabolomics

The relationship between xenobiotic concentration and effect is very important in pharmacology. Consequently, using reference standards, we optimized chromatographic conditions to achieve at least partial separation using a shorter run time and estimated the concentration of the adenosine metabolites present in the App*ΔapxICΔapxIIC* culture supernatant ultrafiltrates. As shown in Figure 6, targeted HPLC-SRM/MS analyses of the App*ΔapxICΔapxIIC* culture supernatant ultrafiltrates and specific adenosine metabolite standards undoubtedly revealed the presence of 2-AMP, 3-AMP, 5-AMP, 2,3-cAMP and 3,5-cAMP in the supernatant. Semiquantification analyses were performed using a calibration curve (0.01–1.0 mM) based on the peak area for each targeted adenosine metabolite prepared in DMEM. The calculated coefficient of determination (R^2) was better than 0.993 for each analyte, as revealed in Figure 7. Three biological replicates of App*ΔapxICΔapxIIC* culture supernatant ultrafiltrate were analyzed in triplicate, and as shown in Figure 7, semiquantification was performed using the calibration curve based on peak area to determine the concentrations. Unexpectedly, we observed that the mean concentrations derived from 3 biological replicates were 0.74 mM for 3-AMP and 0.65 mM for 2,3-cAMP. It is also interesting to note that 2,3-cAMP can be metabolized to 2-AMP and 3-AMP [25]. The others were below 0.1 mM. These semiquantitative analyses were important to set relevant concentrations to test the antiviral activity of the identified adenosine nucleoside metabolites.

3.4 Determination of adenosine nucleoside antiviral activity against PRRSV

The observed high concentrations of adenosine nucleoside metabolites in App*ΔapxICΔapxIIC* culture supernatant ultrafiltrates were unexpected, and further investigation is required to

determine whether these molecules show antiviral activity against PRRSV in SJPL cells. Thus, treatments with 2-AMP, 3-AMP, 5-AMP, 2,3-cAMP and 3,5-cAMP were tested after infection with PRRSV in SJPL cells. As shown in Figure 8A, dose-dependent inhibition of PRRSV replication in SJPL cells was observed for 2-AMP, 3-AMP and 5-AMP but not for 2,3-cAMP and 3,5-cAMP. Interestingly, 2-AMP and 3-AMP have significantly more antiviral effects than 5-AMP. As shown in Figure 8B, these results are strengthened based on the fluorescence intensity computation performed with ImageJ software. As revealed in Figure 2, 3-AMP appears to be the nucleoside with the highest abundance detected in App*ΔapxICΔapxIIC* culture supernatant ultrafiltrates. 2-AMP, 3-AMP and 5-AMP are phosphorylated by cellular nucleoside kinases, resulting in the formation of nucleoside di- and triphosphates. Thus, we believe that the cellular accumulation of nucleoside triphosphate nucleoside species inhibits RNA polymerases. Interestingly, no significant effect was observed for 2,3-cAMP or 3,5-cAMP. However, the cellular degradation of 2,3-cAMP will lead to 2-AMP and 3-AMP, potentially increasing the formation of triphosphate nucleoside species and the inhibition of RNA polymerases. Overall, these investigations strongly support that App*ΔapxICΔapxIIC* culture supernatant ultrafiltrates antiviral effects against PRRSV in SJPL cells are produced mainly by 3-AMP but that 2-AMP and 5-AMP could also contribute seemingly, similar to other detected monophosphate nucleoside species. Interestingly, a recent study using small interfering RNAs (siRNAs) targeting porcine 5′-AMP-activated protein kinase (AMPK) suggested that fatty acids regulate PRRSV infectivity through the AMPK-ACC1 signaling pathway [18]. Although these results are interesting and provide complementary explanations to our previous studies [12–15], the potential application remains questionable. The treatment of PRRSV-infected SJPL cells with App*ΔapxICΔapxIIC* culture supernatant ultrafiltrates led to the exposure of very high concentrations (i.e., ~1 mM) of adenosine metabolites that cannot be realistically translated *in vivo*. No significant effects were

observed at a lower concentration. However, these results may suggest that currently marketed nucleoside analog drugs could be used to treat PRRSV infections. In fact, many marketed antiviral drugs are adenosine analogs [23]. The intracellular uptake and metabolism of nucleoside analogs and nucleoside analog prodrugs is well known [23]. Through viral RNA replication, nucleoside analogs are incorporated into nascent RNA chains, resulting in termination of nucleic acid synthesis or in accumulation of mutations in viral genomes to suppress viral replication due to error. Additionally, the accumulation of nucleoside triphosphate species of nucleoside analogs inhibits RNA polymerases.

4. Conclusion

This study confirmed our previous studies [12–14] that App*ΔapxICΔapxIIC* cultured supernatant ultrafiltrate has an antiviral effect against PRRSV in SJPL cells. Untargeted mass spectrometry-based metabolomics was performed and identified several adenosine metabolites. Further quantification using an HPLC-SRM-MS-based method revealed very high concentrations (~1 mM) of 3-AMP and 2,3-cAMP. All adenosine monophosphate metabolites tested showed significant antiviral effects, but 2-AMP and 3-AMP were more potent. Interestingly, many marketed antiviral drugs or prodrugs are adenosine analogs. Several display interesting results for the treatment of infections with RNA viruses.

Declaration of competing interest

The authors declare that they have no known competing financial interests or personal relationships that could have influenced the work reported in this manuscript.

Acknowledgments

This project was funded by the Swine Innovation Porc (PI: C. Gagnon, Project 1781). Bioanalytical equipment was funded by the Canadian Foundation for Innovation (CFI), the *Fonds*

de Recherche du Québec (FRQ), and the Government of Quebec (PI: F. Beaudry CFI John R. Evans Leaders grant no. 36706).

References

1- Albina E, Epidemiology of porcine reproductive and respiratory syndrome (PRRS): An overview. Vet Res 1997;55(1-4): 309-316.

2- BilodeauR, Dea S, Sauvageau RA and Martineau GP. Porcine reproductive and respiratory syndrome' in Quebec. Vet Rec 1991;129:102-3

3- Christianson WT. Stillbirths, Mummies, Abortions, and Early Embryonic Death. Vet Clin North Am Food Anim Pract 1992;8(3): 623-639

4- Keffaber KK. Reproductive failure of unknown etiology. AASP Newsletter. 1989;2:1-10.

5- Loula T. Mystery pig disease. Agri-Practice 1991;12: 23-34

6- Pol JM, van Dijk JE, Wensvoort G, Terpstra C. Pathological, ultrastructural, and immunohistochemical changes caused by Lelystad virus in experimentally induced infections of mystery swine disease (synonym: porcine epidemic abortion and respiratory syndrome (PEARS)). Vet Q 1991; 13(3):137-143

7- Chand RJ, Trible BR and Rowland RRR. Pathogenesis of porcine reproductive and respiratory syndrome virus Current Opinion in Virology 2012; 2 (3): 256.

8- Dorr PM, Gebreyes WA, Almond GW. Porcine reproductive and respiratory syndrome virus: Age and management system disease modeling for pathogenic co-infection. J Swine Health Prod. 2007;15(5):258–263

9- Lunney JK, Fang Y, Ladining A, Chen N, Li Y, Rowland B, Renukaradhya GJ. Porcine Reproductive and Respiratory Syndrome Virus (PRRSV): Pathogenesis and Interaction with the Immune System. Annu Rev Anim Biosci 2016;4:129-154.

10- Kimman TG, Cornelissen LA, Moormann RJ, Rebel JM, Stockhofe-Zurwieden N.Challenges for porcine reproductive and respiratory syndrome virus (PRRSV) vaccinologyVaccine 2009; 27(28):3704-3718

11- Auger E, Deslandes V, Ramjeet M, Contreras I, Nash JH, Harel J, Gottschalk M, Olivier M, Jacques M. Infect Immun. 2009;77(4):1426-1441.

12- Lévesque C., Provost C, Labrie J, Hernandez Reyes Y, Burciaga Nava JA, Gagnon CA, Jacques M. Actinobacillus pleuropneumoniae Possesses an Antiviral Activity against Porcine Reproductive and Respiratory Syndrome Virus. PLoS One. 2014:9;e98434-11.

13- Reyes YH, Provost C, Traesel CK, Jacques M and Gagnon CA. Actinobacillus pleuropneumoniae culture supernatant antiviral effect against porcine reproductive and respiratory syndrome virus occurs prior to the viral genome replication and transcription through actin depolymerization. J Med Microbiol. 2018:67; 249–264.

14- Barbosa JA., Labrie J, Beaudry F, Gagnon CA and Jacques M. Actinobacillus pleuropneumoniae induces SJPL cell cycle arrest in G2/M-phase and inhibits porcine reproductive and respiratory syndrome virus replication. Virology Journal. 2015;12:188

15- Wang G, Yu Y, He X, Wang M, Cai X, Zimmerman JJ. Porcine reproductive and respiratory syndrome virus infection of bone marrow: Lesions and pathogenesis. Virus Res. 2019;265:20-29

16- Saade G, Deblanc C, Bougon J, Marois-Créhan C, Fablet C, Auray G, Belloc C, Leblanc-Maridor M, Gagnon CA, Zhu J, Gottschalk M, Summerfield A, Simon G, Bertho N, Meurens F. Coinfections and their molecular consequences in the porcine respiratory tract. Vet Res. 2020;51(1):80.

17- Salguero FJ, Frossard JP, Rebel JM, Stadejek T, Morgan SB, Graham SP, Steinbach F. Host-pathogen interactions during porcine reproductive and respiratory syndrome virus 1 infection of piglets. Virus Res. 2015;202:135-43

18. Long S, Zhou Y, Bai D, Hao W, Zheng B, Xiao S, Fang L. Fatty Acids Regulate Porcine Reproductive and Respiratory Syndrome Virus Infection via the AMPK-ACC1 Signaling Pathway. Viruses. 2019;11(12):1145.

19- Tremblay YDN, Lévesque C, Segers RPAM, Jacques M. Method to grow Actinobacillus pleuropneumoniae biofilm on a biotic surface. BMC Vet Res. 2013;9:213.

20- Mardassi H, Athanassious R, Mounir S, Dea S. Porcine reproductive andrespiratory syndrome virus: morphological, biochemical and serologicalcharacteristics of Québec isolates associated with acute and chronicoutbreaks of porcine reproductive and respiratory syndrome. Can J Vet Res.1994;58:55–64.

21- Gagnon CA, Lachapelle G, Langelier Y, Massie B, Dea S. Adenoviral-expressedGP5 of porcine respiratory and reproductive syndrome virus differs in itscellular maturation from the authentic viral protein but maintains knownbiological functions. Arch Virol. 2003;148:951–972.

22- Schneider CA, Rasband WS, Eliceiri KW. NIH Image to ImageJ: 25 years of image analysis. Nat Methods. 2012;9(7): 671–675.

23- Eyer L, Nencka R, Clercq E, Seley-Radtke K. and Růžek D. Nucleoside analogs as a rich source of antiviral agents active against arthropod-borne flaviviruses. Antivir Chem Chemother 2018;26:1-28

List of Figures

Figure 1. Immunofluorescence detection of PRRSV in SJPL-infected and treated cells. A. Representative immunofluorescence images were acquired at 100 × magnification. B.

Fluorescence intensity was computed from microscopy results using ImageJ software. A minimum of 50 cells per field was used to compute the fluorescence intensity. Mean fluorescence values ± SD are display. The results show that the *App* culture supernatant ultrafiltrate has a significant antiviral effect. ANOVA–Dunnett's multiple comparison versus the PRRSV-infected group. **** $p < 0.0001$.

Figure 2. Nontargeted differential screening of metabolites present in App*ΔapxICΔapxIIC* culture supernatant using HPLC-HRAM-MS. Unbiased nontargeted screening of combined full scan (MS^1) and data-dependent Top-6 (MS^2) data was performed. **A**. Data are presented as log2 fold-change in relative abundance of untargeted metabolites. Only metabolites with positive identification from mzCloud, mzVault or ChemSpider are displayed. A total of 1075 metabolites were identified. Several nucleoside metabolites, including adenosine nucleosides, were among the top 100 most abundant metabolites present in the App*ΔapxICΔapxIIC* culture supernatant (green dot: 3-AMP; orange dot: camp; blue dots: other nucleosides). **B**. Extracted ion chromatogram (XIC) m/z 348.07036 +/- 5 ppm. This ion is highly abundant in App*ΔapxICΔapxIIC* culture supernatant and absent in DMEM. **C**. MS^2 spectrum of m/z 348.07036. Compound identification was performed using a semiautomatic stepwise approach employing an experimental MS^2 fragmentation database, mzCloud reference spectra database and *in silico* predicted fragmentation. As shown, one of the most abundant components was adenosine 3'-monophosphate (3-AMP).

Figure 3. High-resolution mass spectrometry analysis of selected adenosine nucleoside reference standards. Extracted ion chromatogram (XIC) m/z 348.07036 +/- 5 ppm (2-AMP, 3-AMP and 5-AMP) or 330.05980 +/- 5 ppm (2,3-cAMP and 3,5-cAMP), MS^1 and MS^2 spectra are displayed.

Figure 4. Proposed MS^2 fragmentation products. **A**. MS^2 principal product ions for adenosine monophosphate metabolites (2-AMP, 3-AMP and 5-AMP). **B**. MS^2 principal product ions for cyclic adenosine monophosphate metabolites (2,3-cAMP and 3,5-cAMP)

Figure 5. Identification of highly abundant metabolites present in App*ΔapxICΔapxIIC* culture supernatant using HPLC-HRAM-MS. **A**. Full-scan total ion chromatogram (m/z 75–1000). **B**. Extracted ion chromatogram (XIC) m/z 348.07036 +/- 5 ppm. **C**. Extracted ion chromatogram (XIC) m/z 330.05980 +/- 5 ppm. **D**. Product ion spectra of m/z 348. **E**. Product ion spectra of m/z 330. The MS^1 and MS^2 spectra are consistent with adenosine monophosphate and cyclic adenosine monophosphate metabolites.

Figure 6. Targeted analysis of adenosine nucleosides using HPLC-SRM/MS. **A**. SRM chromatogram (348→136) of 5-AMP, 3-AMP and 2-AMP reference standards (1 mM). As shown, all three nucleosides were separated. **B**. SRM chromatogram (348→136) of App*ΔapxICΔapxIIC* culture supernatant ultrafiltrate. The intensity of 3-AMP was significantly higher, but 2-AMP and 5-AMP were detected. **C**. SRM chromatogram (330→136) of 3,5-cAMP and 2,3-cAMP reference standards (1 mM). As shown, 3,5-cAMP and 2,3-cAMP were separated. **D**. SRM chromatogram (330→136) of App*ΔapxICΔapxIIC* culture supernatant ultrafiltrate. The observed intensity of 2,3-cAMP is significantly higher than that of 3,5-cAMP."

Figure 7. Calibration curve for targeted adenosine nucleosides and semiquantitative analysis in App*ΔapxICΔapxIIC* culture supernatants using HPLC-SRM/MS.

Figure 8. Immunofluorescence detection of PRRSV in SJPL-infected and SJPL-treated cells with specific adenosine metabolites. **A**. Representative immunofluorescence images were acquired at 100 × magnification. **B**. Fluorescence intensity was computed from microscopy results using ImageJ software. A minimum of 50 cells per field was used to compute the fluorescence intensity. Mean fluorescence values ± SD are displayed. The results showed a significant reduction in fluorescence following treatment with 2-AMP, 3-AMP and 5-AMP. No noticeable effects were noted for 2,3-cAMP and 3,5-cAMP. ANOVA–Dunnett's multiple comparison versus the PRRSV-infected group. ** $p < 0.01$, **** $p < 0.0001$.

Figure 1.

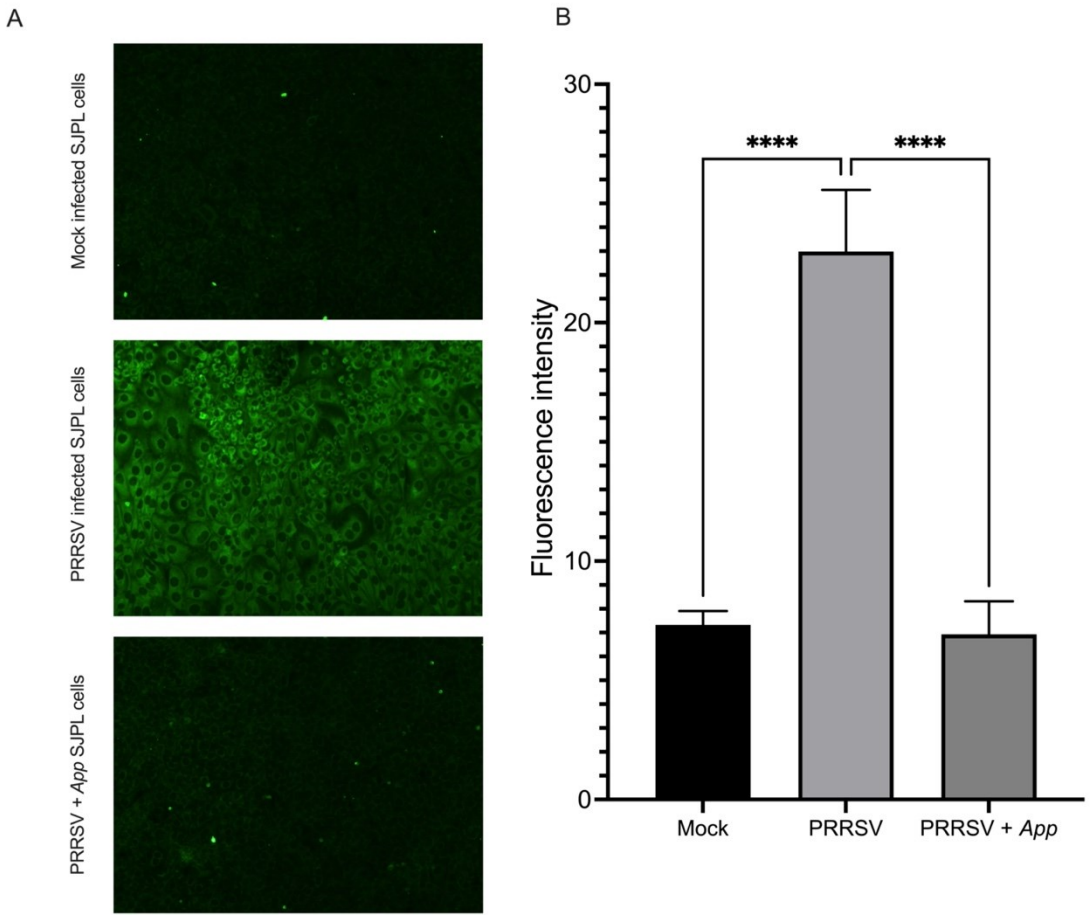
A
Mock infected SJPL cells
PRRSV infected SJPL cells
PRRSV + App SJPL cells
B
Fluorescence intensity
30
20
10
0
****
****
Mock
PRRSV
PRRSV + App

Figure 2.

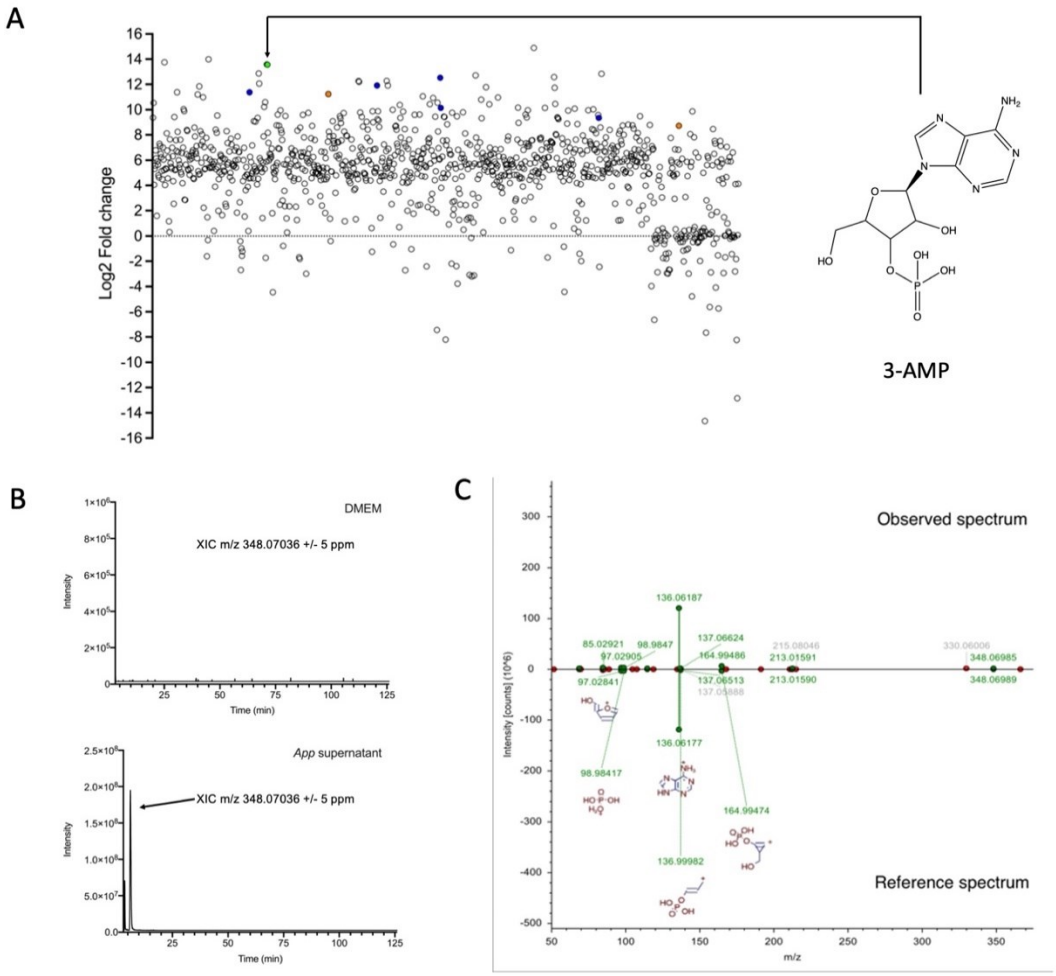
A
Log2 Fold change
3-AMP
B
DMEM
XIC m/z 348.07036 +/- 5 ppm
Intensity
Time (min)
App supernatant
XIC m/z 348.07036 +/- 5 ppm
C
Observed spectrum
Reference spectrum
Intensity [counts] (10^6)
m/z

Figure 3.

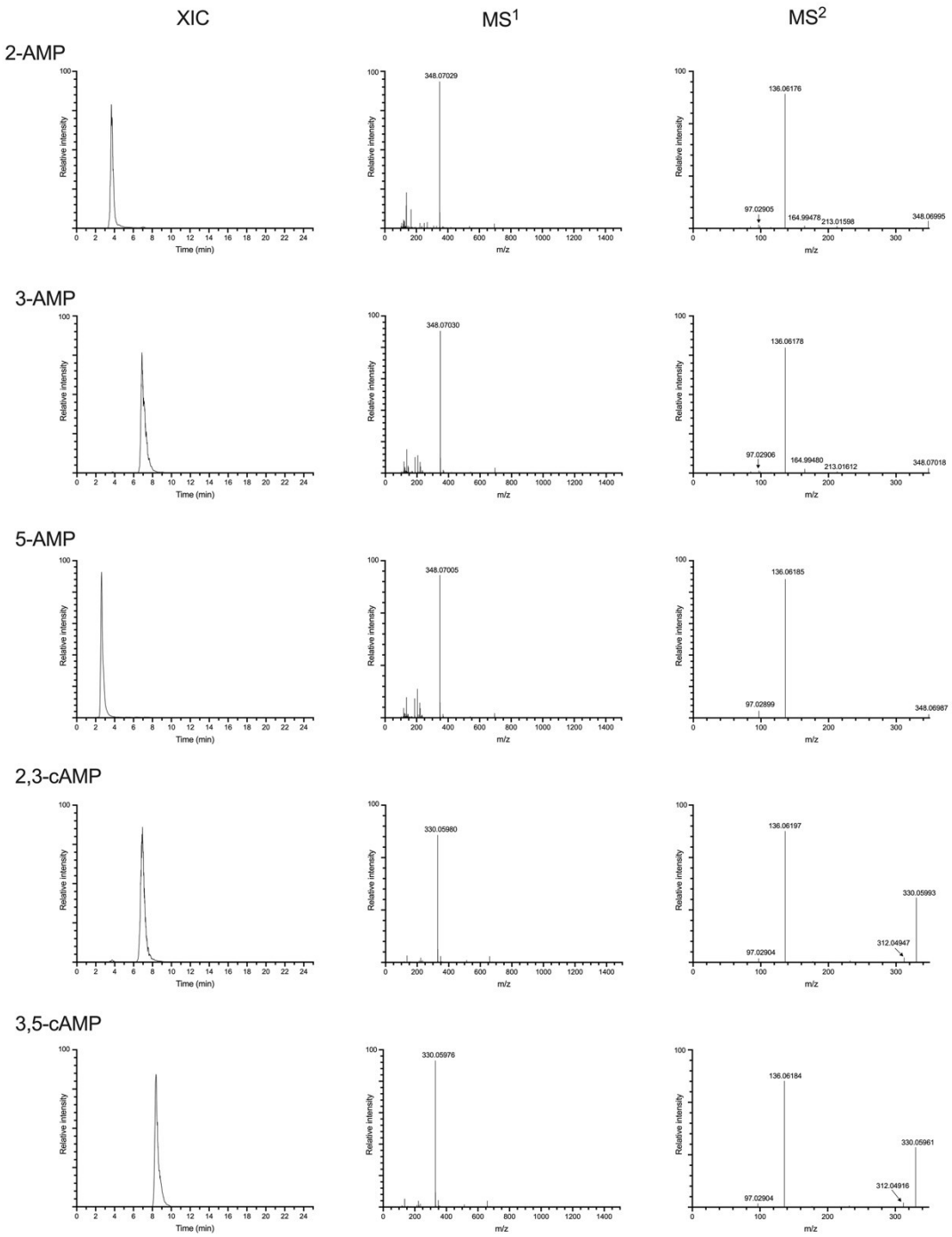
XIC
MS1
MS2
2-AMP
3-AMP
5-AMP
2,3-cAMP
3,5-cAMP
Relative intensity
Time (min)
m/z
348.07029
136.06176
97.02905
164.99478
213.01598
348.06995
348.07030
136.06178
97.02906
164.99480
213.01612
348.07018
348.07005
136.06185
97.02899
348.06987
330.05980
136.06197
330.05993
312.04947
97.02904
330.05976
136.06184
330.05961
312.04916
97.02904

Figure 4.

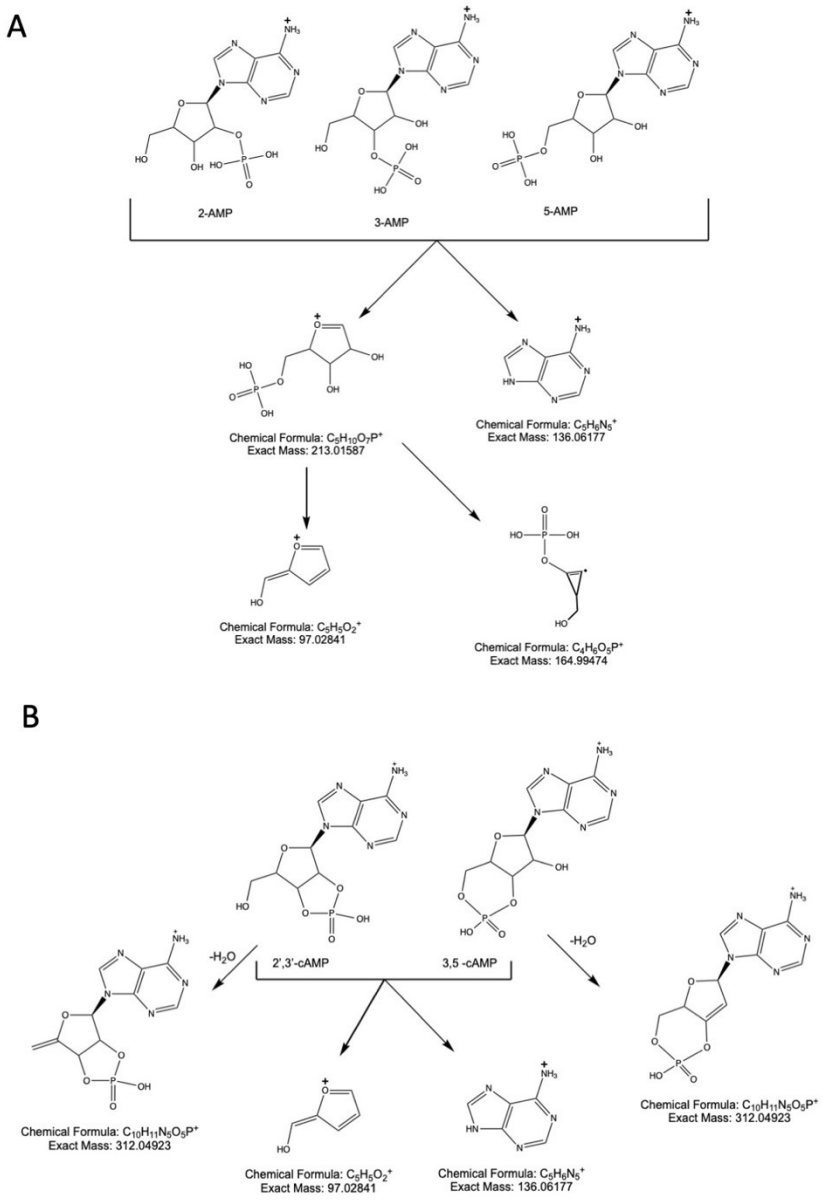
A
2-AMP
3-AMP
5-AMP
Chemical Formula: $C_5H_{10}O_7P^+$
Exact Mass: 213.01587
Chemical Formula: $C_5H_6N_5^+$
Exact Mass: 136.06177
Chemical Formula: $C_5H_5O_2^+$
Exact Mass: 97.02841
Chemical Formula: $C_4H_6O_5P^+$
Exact Mass: 164.99474
B
-H_2O
2',3'-cAMP
3,5 -cAMP
-H_2O
Chemical Formula: $C_{10}H_{11}N_5O_9P^+$
Exact Mass: 312.04923
Chemical Formula: $C_5H_5O_2^+$
Exact Mass: 97.02841
Chemical Formula: $C_5H_6N_5^+$
Exact Mass: 136.06177
Chemical Formula: $C_{10}H_{11}N_5O_9P^+$
Exact Mass: 312.04923

Figure 5.

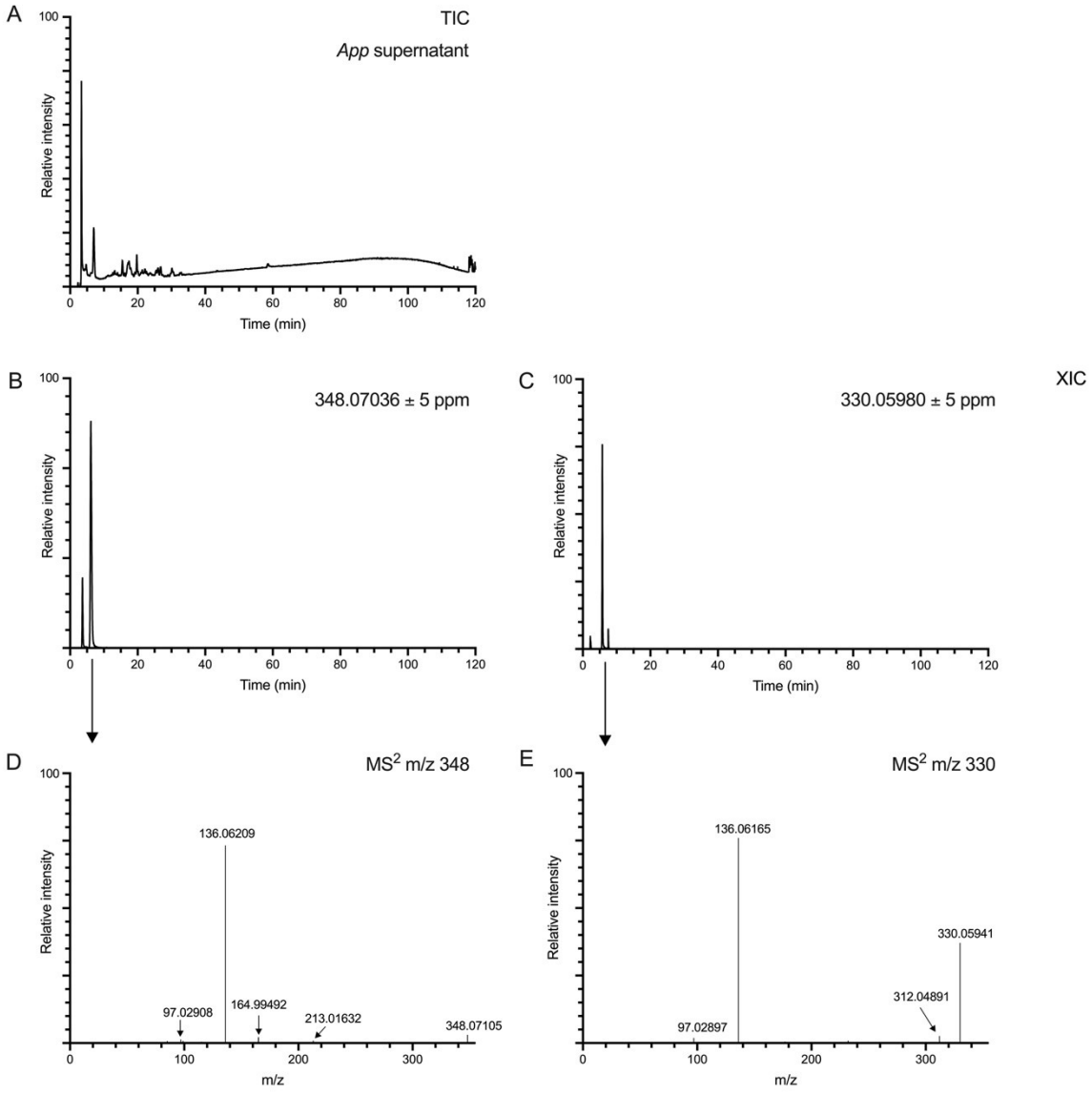
A
TIC
App supernatant
Relative intensity
Time (min)
B
348.07036 ± 5 ppm
C
330.05980 ± 5 ppm
XIC
D
MS2 m/z 348
136.06209
97.02908
164.99492
213.01632
348.07105
m/z
E
MS2 m/z 330
136.06165
330.05941
312.04891
97.02897

Figure 6.

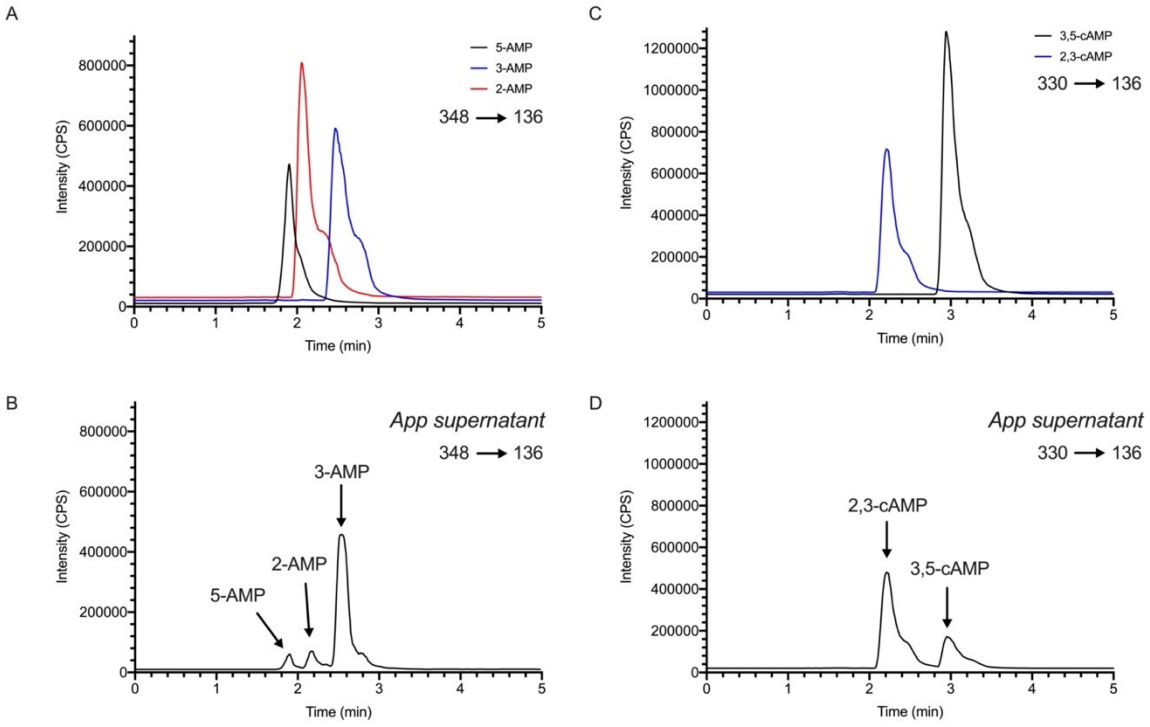
A
5-AMP
3-AMP
2-AMP
348 → 136
Intensity (CPS)
Time (min)
C
3,5-cAMP
2,3-cAMP
330 → 136
Intensity (CPS)
Time (min)
B
App supernatant
348 → 136
3-AMP
2-AMP
5-AMP
Intensity (CPS)
Time (min)
D
App supernatant
330 → 136
2,3-cAMP
3,5-cAMP
Intensity (CPS)
Time (min)

Figure 7.

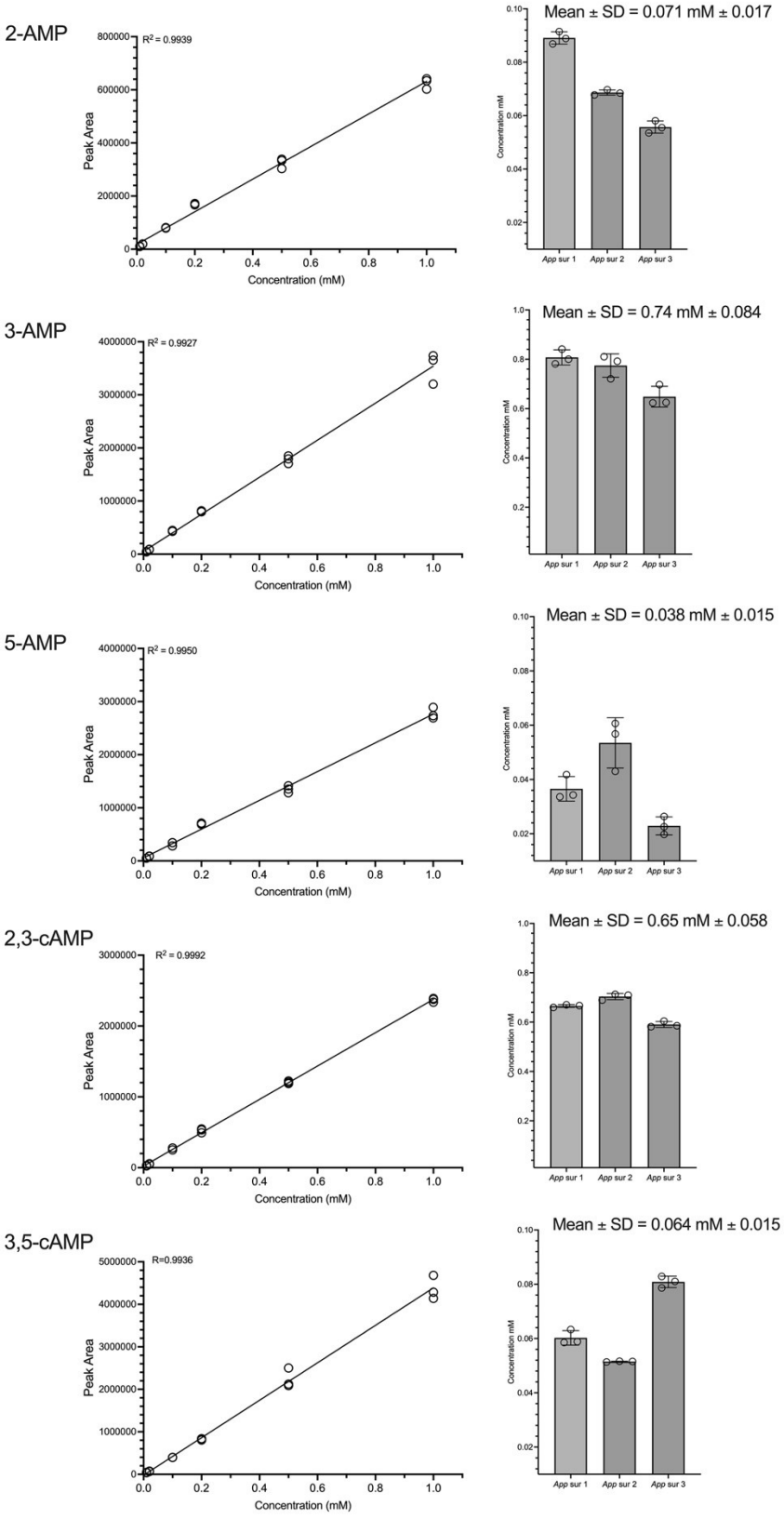
2-AMP
R² = 0.9939
Peak Area
Concentration (mM)
Mean ± SD = 0.071 mM ± 0.017
Concentration mM
App sur 1
App sur 2
App sur 3
3-AMP
R² = 0.9927
Peak Area
Concentration (mM)
Mean ± SD = 0.74 mM ± 0.084
Concentration mM
App sur 1
App sur 2
App sur 3
5-AMP
R² = 0.9950
Peak Area
Concentration (mM)
Mean ± SD = 0.038 mM ± 0.015
Concentration mM
App sur 1
App sur 2
App sur 3
2,3-cAMP
R² = 0.9992
Peak Area
Concentration (mM)
Mean ± SD = 0.65 mM ± 0.058
Concentration mM
App sur 1
App sur 2
App sur 3
3,5-cAMP
R=0.9936
Peak Area
Concentration (mM)
Mean ± SD = 0.064 mM ± 0.015
Concentration mM
App sur 1
App sur 2
App sur 3

Figure 8.

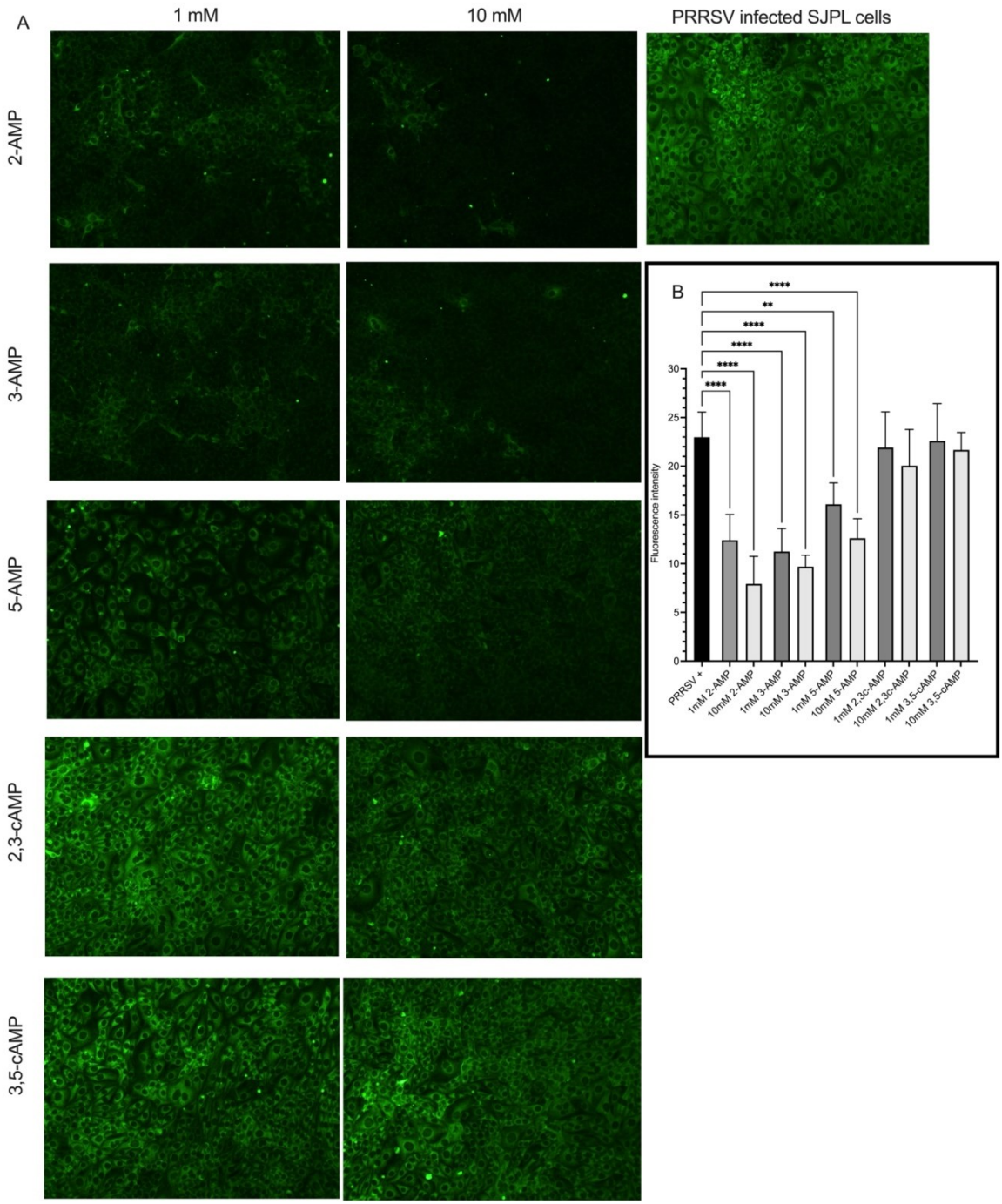
A
1 mM
10 mM
PRRSV infected SJPL cells
2-AMP
3-AMP
5-AMP
2,3-cAMP
3,5-cAMP
B
Fluorescence intensity
PRRSV +
1mM 2-AMP
10mM 2-AMP
1mM 3-AMP
10mM 3-AMP
1mM 5-AMP
10mM 5-AMP
1mM 2,3c-AMP
10mM 2,3c-AMP
1mM 3,5-cAMP
10mM 3,5-cAMP

GENERAL DISCUSSION

PRRSV is a worldwide endemic disease which causes millions in financial losses annually in pig producing countries [1]. *App* is the causative agent of porcine pleuropneumonia, a disease responsible for major economic losses in the swine industry worldwide [11]. During respiratory tract infections pigs are often colonized by more than one viral/bacterial pathogen at a time, this phenomenon is known as PRDC [10]. *App* and PRRSV are pathogens that are frequently involved in PRDC [15].

Since co-infections are likely more common than reported in the field, and that a primary infection with a viral or bacterial pathogen may enhance the infectious potential of a secondary pathogen, *in vitro* studies were launched in our group to investigate the interactions between *App* and PRRSV [12-14, 51]. Using multiple cell lines, namely the St Jude porcine lung (SJPL), MARC-145 and porcine alveolar macrophage (PAM) cell lines, it was observed that *App* culture supernatants have strong antiviral activity against PRRSV, during *App*-PRRSV co-infections of SJPL cells [12-14].

PRRSV can lead to persistent infections [113, 114]and current PRRSV vaccines are not yet optimal, since they lack the ability to induce a strong immune response and since they do not provide complete immunity against heterologous PRRSV infections [115, 116]. Moreover, most PRRSV vaccines are live attenuated virus and thus present a safety issue; some vaccinated pigs were shown to shed virulent PRRSV particles [117]. Thus, it is important to further investigate new possible ways to control PRRSV infections. In that regards, an antiviral molecule or metabolite might be a good alternative to the currently used vaccines.

The main objective of the current study was to identify the unknown metabolites present in the *App* supernatant that are responsible for the antiviral effect against PRRSV. In order to achieve this objective, we had to run multiple high resolution mass spectrometry experiments on our active *App* cell culture supernatant. This experiment revealed that multiple metabolites are present in *App* cell culture supernatant which have been shown to have antiviral effects against a multitude of viruses and the mechanism in which those metabolites function have been elaborated in previous studies.

Summary of results

SJPL is a PRRSV permissive cell line specifically used to test *AppΔapxICΔapxIIC* antiviral activity as revealed in previous studies [12-14]. Treatment with *AppΔapxICΔapxIIC* culture supernatant ultrafiltrates (i.e. < 3KDa) was performed after infection with PRRSV in SJPL cells. PRRSV antigen detection in SJPL using IFA revealed that *AppΔapxICΔapxIIC* culture supernatant significantly inhibits PRRSV replication. These results were confirmed based on the fluorescence intensity computation performed with ImageJ software and are coherent with previous studies[12-14].

In order to identify the molecules responsible for the *AppΔapxICΔapxIIC* culture supernatant ultrafiltrates antiviral effect, we first used an untargeted metabolomic strategy using a Hybrid Orbitrap HPLC-MS system and a Data-dependent acquisition (DDA) mode. Untargeted metabolomics is challenging because it aims at identifying and quantifying hundreds to thousands of different compounds with various chemical properties and structure with limited prior knowledge of the metabolites. It is, therefore, advantageous to use a mass spectrometer system that provides accurate mass information for confident confirmation and structural elucidation. Differential bioinformatic analyses were performed using Thermo Scientific Compound Discoverer 3.1 performing background subtraction, component detection, peak alignment, and differential analysis. Identifications were based on MS^1 and MS^2 mass spectral database matching (i.e. mzCloud and ChemSpider). The untargeted DDA TOP-6 analysis of molecules present in *AppΔapxICΔapxIIC* culture supernatant ultrafiltrates revealed the presence of several nucleoside metabolites. More specifically, in the TOP-5 most abundant (i.e. based on $\log_2$ fold-change), we found 3'-Adenylic acid (3-AMP). Extracted ion chromatograms (m/z 348.07036 $\pm$ 5 ppm) comparing the control sample (DMEM) and the *AppΔapxICΔapxIIC* culture supernatant ultrafiltrates showed an absence of 3-AMP in the control but very high concentration in the *AppΔapxICΔapxIIC* culture supernatant ultrafiltrates. Furthermore, MS^2 spectra data comparing observed spectrum and curated reference spectrum extracted from mzCloud strongly supported the identification of 3-AMP.

Consequently, using reference standards, we evaluated the concentration of the adenosine metabolites present in the *AppΔapxICΔapxIIC* culture supernatant ultrafiltrates. Using targeted HPLC-SRM/MS analyses of the *AppΔapxICΔapxIIC* culture supernatant ultrafiltrates and specific adenosine metabolites standards undoubtedly revealed the presence of 2-AMP, 3-AMP, 5-AMP, 2,3-cAMP and 3,5-cAMP in the supernatant. The adenosine metabolites standards were injected at a concentration of 1 mM and semi-quantification based on the peak area suggested concentrations of 0.78 mM for 3-AMP and 0.67 mM for 2,3-cAMP.

Thus, treatment with 2-AMP, 3-AMP, 5-AMP, 2,3-cAMP and 3,5-cAMP was tested after infection with PRRSV in SJPL cells. We used doses of 1mM and 10mM and noticed a dose-dependent inhibition effect of PRRSV replication in SJPL cells for 2-AMP, 3-AMP and 5-AMP, but not for 2,3-cAMP and 3,5-cAMP. Interestingly, 2-AMP and 3-AMP have shown significantly more antiviral effects when compared to 5-AMP. These results are strengthened based on the fluorescence intensity computation performed with ImageJ software.

Relevance of observations

Unequivocally, the results obtained from this study and previous studies [12-14] strongly supported that low molecular weight metabolites were potentially responsible for the antiviral activity of the *App* supernatant.

Using high resolution mass spectrometry, multiple adenosine nucleoside metabolites (i.e 2-AMP, 5-AMP, 2,3-cAMP and 3,5-cAMP) and other nucleosides were detected at very high concentrations. The MS analysis revealed that 3-AMP was the nucleoside metabolite with the highest abundance detected in *AppΔapxICΔapxIIC* culture supernatant ultrafiltrates. These results were unexpected but highly interesting since a wide variety of adenosine nucleoside analogs and prodrugs are currently available and show antiviral activity against several RNA viruses [108, 112]. Moreover, it is important to note, nucleoside analogs constitute the main class of small molecule-based antivirals available on the market or under investigation.

The relationship between xenobiotic concentration and effect is very important in pharmacology. The observed high concentrations of adenosine nucleoside metabolites in

AppΔapxICΔapxIIC culture supernatant ultrafiltrates were unexpected and further investigation was required to determine if these molecules showed a dose dependent antiviral activity against PRRSV in SJPL cells individually. Interactions between two or more of the metabolites might have had a total effect that is greater than the sum of the individual effects of each metabolite by itself. The semi-quantitative analysis allowed us to set relevant concentrations for the identified adenosine nucleoside metabolites, we then used the same protocols that were utilized for our *App* supernatant for antiviral activity testing.

2-AMP, 3-AMP and 5-AMP are phosphorylated by cellular nucleoside kinases resulting in formation of nucleoside di-, and triphosphates. Thus, we believe that the cellular accumulation of nucleoside triphosphates species is inhibiting RNA polymerases. Interestingly, no significant effect is observed for 2,3-cAMP or 3,5-cAMP. However, it is noteworthy to mention that 2,3-cAMP can be metabolized to 2-AMP and 3-AMP [118], potentially increasing the formation of triphosphates nucleoside species and the inhibition of RNA polymerases [118].

The results we obtained from our current study have been unexpected, however they are coherent with our previous research results [12, 13]. Reyes et al 2018[13], hypothesized that the antiviral activity maybe due to actin depolymerization through the activation of cofilin, interestingly there have been multiple studies done exhibiting the interactions of different viruses with the actin cytoskeleton [84, 85], one of the studies showed that there is an increase of actin and tubulin on the surface of the cells infected with EBV [85]. Another study revealed that the binding affinity of cofilin increased at cellular levels with increased levels of ATP [119]. This further reinforces our theory of the accumulation of nucleoside triphosphates within the cells.

Interestingly, the molecular identification results obtained were compatible with Barbosa *et al* (2015) [14]. The analysis of MS^1 spectra displayed in Figure 9 and unpublished MS^2 spectra reveal the molecules extracted from the TLC spot and analyzed by MS were compatible with secondary metabolites derived from 2-AMP, 3-AMP or 5-AMP. The peak observed at m/z 515 were compatible with the addition of phosphoserine and the MS^2 spectra shows a neutral loss of 167 Da compatible with a phosphoserine on 2-AMP, 3-AMP or 5-AMP [120].

Interestingly, phosphoseryladenosine was previously identified resulting from tRNA biotransformation [121-123].

Overall, this investigation strongly supports that *AppΔapxICΔapxIIC* culture supernatant ultrafiltrates antiviral effects against PRRSV in SJPL cells are produced mainly by 3-AMP, but that 2-AMP and 5-AMP could also contribute seemingly like other detected monophosphate nucleoside species. Interestingly, a recent study using small interfering RNAs (siRNAs) targeting porcine 5'-AMP-activated protein kinase (AMPK) suggested fatty acids regulate PRRSV infectivity through the AMPK-ACC1 signaling pathway [124]. An imbalance in AMPK activity has been associated with various chronic diseases including metabolic syndrome, obesity, stress, type II diabetes, or even reduced longevity and the promotion of cancer [124]. Due to its significance, AMPK has been considered a potential target in the treatment of multiple diseases. In this study the investigators revealed that PRRSV infection dramatically increased the levels of phosphorylated AMPK (active form), which antagonized PRRSV replication [124].

Implication of the results

Despite our results, the potential application of our findings remains questionable. The treatment of PRRSV infected SJPL cells with our *App* cell culture supernatant ultrafiltrate leads to the exposure of extremely high concentration of adenosine metabolites (~1mM) which cannot be realistically translated *in vivo.*

Nonetheless, these results may suggest currently marketed nucleoside analog drugs could be used to treat PRRSV infections. In fact, multiple marketed antiviral drugs are adenosine analogs [91, 112]. The intracellular uptake and metabolism of nucleoside analogs and nucleoside analog prodrugs is well known [112]. Through viral RNA replication, nucleoside analogs are incorporated into nascent RNA chains resulting in termination of nucleic acid synthesis or in accumulation of mutations in viral genomes to suppress viral replication due to error. Additionally, the accumulation of nucleoside triphosphates species of nucleoside analogs inhibits RNA polymerases. The current study has provided us with exciting knowledge on perhaps new approaches to combat PRRSV. However, further studies need to be done to assess

the applicability of our findings to promote their subsequent transfer to end-users (swine producers). The *in vivo* efficacy in swine and the economic sustainability of using commercially available nucleoside analog treatments needs to be explored.

Limitations

In order to test the *in vivo* efficacy of adenosine analogs, the concentrations would have to be reduced significantly. This may be achieved by testing marketed adenosine nucleoside drugs and prodrugs such as Adefovir, Tenofovir disoproxil and Remdesivir *in vitro* at acceptable concentrations i.e not higher than 100µM. These three are adenosine analogs, Remdesivir has been shown to have broad spectrum antiviral activity, whereas Adefovir, Tenofovir disoproxil are used for the treatment of Hepatitis-B and HIV-1 infections [86, 89]. If promising results are obtained using the *in vitro* model, an *in vivo* study would be the next step.

Further, the results obtained in this study were quantified using only IFA imagery and the ImageJ software, more accurate results could have been obtained by measuring viral loads pre and post treatment using RT-qPCR. Future *in vitro* studies performed using marketed drugs and prodrugs should utilize both IFA imagery and RT-qPCR for a more accurate measure of the antiviral efficacy as previously reported by Reyes et al 2018 [13]. If these conditions are met, an *in vivo* study maybe launched to determine the feasibility of this approach.

As a veterinarian there are two issues which should be considered when prescribing drugs for extra-label use, especially in food producing animals. Firstly, the safety of the drug, in companion (non-food-producing) animals it is allowed by the food and drugs administration (FDA) to prescribe an approved human drug for an extra-label use even if an approved animal drug is available. However, this is not the case for food-producing animals. For these animals, the FDA prohibits prescribing an approved human drug if there's a drug approved for food-producing animals that can be prescribed instead. For example, if a drug approved for chickens is available, you must first use that drug to treat a sick animal from another species before reaching for a drug approved for humans. Additionally, if scientific information is unavailable on the safety of food products made from animals treated with the drug, appropriate measures

must be taken to ensure that the animal and its food products will not enter the human food supply for obvious reasons.

The second issue to address would be the practicality of using these nucleoside drugs and prodrugs on livestock. As we have shown in this study there is a dose dependent antiviral effect, and the dose required for therapeutic effect is extremely high, this has multiple impacts to consider. Firstly, the economic impact on the producers and consumers, the producers would have increased costs of production which would translate to increased prices for the consumers. Humans would be willing to pay large fees in order become healthy and to remain healthy. However, the fact is farms are businesses, and they aim to be cost effective in order to maximize profits. If treatment with nucleoside analog drugs and prodrugs proves to be economically inefficient, I believe that most producers if not all would consider using alternative methods of combatting PRRSV which are more cost efficient. Another aspect to consider is the impact on the animal itself, would an extremely high dose be safe for the animal's physiology. There are also the environmental impacts to consider, what is the environmental cost of producing these drugs at a high volume for animal treatment.

Bibliographical references

1. Albina, E., *[Porcine reproductive and respiratory syndrome: ten years of experience (1986-1996) with this undesirable viral infection].* Vet Res, 1997. **28**(4): p. 305-52.
2. Bilodeau, R., et al., *'Porcine reproductive and respiratory syndrome' in Quebec.* Vet Rec, 1991. **129**(5): p. 102-3.
3. Christianson, W.T., *Stillbirths, mummies, abortions, and early embryonic death.* Vet Clin North Am Food Anim Pract, 1992. **8**(3): p. 623-39.
4. E, A., *Le point sur le dernier-né des Arterivirus : le virus du syndrome dysgénésique et respiratoire procin (SDRP).* Virologie, 2000. **4**(2): p. 113-21.
5. Pol, J.M., et al., *Pathological, ultrastructural, and immunohistochemical changes caused by Lelystad virus in experimentally induced infections of mystery swine disease (synonym: porcine epidemic abortion and respiratory syndrome (PEARS)).* Vet Q, 1991. **13**(3): p. 137-43.
6. Chand, R.J., B.R. Trible, and R.R. Rowland, *Pathogenesis of porcine reproductive and respiratory syndrome virus.* Curr Opin Virol, 2012. **2**(3): p. 256-63.
7. Dorr, P.M., W.A. Gebreyes, and G.W. Almond, *Porcine reproductive and respiratory syndrome virus: Age and management system disease modeling for pathogenic co-infection.* Journal of Swine Health and Production, 2007. **15**(5): p. 258-264.
8. Lunney, J.K., et al., *Porcine Reproductive and Respiratory Syndrome Virus (PRRSV): Pathogenesis and Interaction with the Immune System.* Annu Rev Anim Biosci, 2016. **4**: p. 129-54.
9. Kimman, T.G., et al., *Challenges for porcine reproductive and respiratory syndrome virus (PRRSV) vaccinology.* Vaccine, 2009. **27**(28): p. 3704-18.
10. Saade, G., et al., *Coinfections and their molecular consequences in the porcine respiratory tract.* Vet Res, 2020. **51**(1): p. 80.
11. Auger, E., et al., *Host-pathogen interactions of Actinobacillus pleuropneumoniae with porcine lung and tracheal epithelial cells.* Infect Immun, 2009. **77**(4): p. 1426-41.
12. Lévesque, C., et al., *Actinobacillus pleuropneumoniae possesses an antiviral activity against porcine reproductive and respiratory syndrome virus.* PLoS One, 2014. **9**(5): p. e98434.
13. Hernandez Reyes, Y., et al., *Actinobacillus pleuropneumoniae culture supernatant antiviral effect against porcine reproductive and respiratory syndrome virus occurs prior to the viral genome replication and transcription through actin depolymerization.* J Med Microbiol, 2018. **67**(2): p. 249-264.
14. Ferreira Barbosa, J.A., et al., *Actinobacillus pleuropneumoniae induces SJPL cell cycle arrest in G2/M-phase and inhibits porcine reproductive and respiratory syndrome virus replication.* Virol J, 2015. **12**: p. 188.
15. Woeste, K. and E. Grosse Beilage, *[Transmission of agents of the porcine respiratory disease complex (PRDC) between swine herds: a review. Part 1--diagnosis, transmission by animal contact].* Dtsch Tierarztl Wochenschr, 2007. **114**(9): p. 324-6, 328-37.
16. Brockmeier, S.L., P.G. Halbur, and E.L. Thacker, in *Polymicrobial Diseases*. 2002, ASM Press: Washington (DC).

17. Chae, C., *Porcine respiratory disease complex: Interaction of vaccination and porcine circovirus type 2, porcine reproductive and respiratory syndrome virus, and Mycoplasma hyopneumoniae.* Vet J, 2016. **212**: p. 1-6.
18. Cho, J.G. and S.A. Dee, *Porcine reproductive and respiratory syndrome virus.* Theriogenology, 2006. **66**(3): p. 655-662.
19. Wensvoort, G., et al., *Mystery swine disease in The Netherlands: the isolation of Lelystad virus.* Vet Q, 1991. **13**(3): p. 121-30.
20. Benfield, D.A., et al., *Characterization of swine infertility and respiratory syndrome (SIRS) virus (isolate ATCC VR-2332).* J Vet Diagn Invest, 1992. **4**(2): p. 127-33.
21. Neumann, E.J., et al., *Assessment of the economic impact of porcine reproductive and respiratory syndrome on swine production in the United States.* J Am Vet Med Assoc, 2005. **227**(3): p. 385-92.
22. Allende, R., et al., *North American and European porcine reproductive and respiratory syndrome viruses differ in non-structural protein coding regions.* J Gen Virol, 1999. **80 (Pt 2)**: p. 307-315.
23. Nelsen, C.J., M.P. Murtaugh, and K.S. Faaberg, *Porcine reproductive and respiratory syndrome virus comparison: divergent evolution on two continents.* J Virol, 1999. **73**(1): p. 270-80.
24. Plagemann, P.G., *Porcine reproductive and respiratory syndrome virus: origin hypothesis.* Emerg Infect Dis, 2003. **9**(8): p. 903-8.
25. Han, J., Y. Wang, and K.S. Faaberg, *Complete genome analysis of RFLP 184 isolates of porcine reproductive and respiratory syndrome virus.* Virus Res, 2006. **122**(1-2): p. 175-82.
26. Meng, X.J., et al., *Characterization of a high-virulence US isolate of porcine reproductive and respiratory syndrome virus in a continuous cell line, ATCC CRL11171.* J Vet Diagn Invest, 1996. **8**(3): p. 374-81.
27. Meng, X.J., et al., *A nested set of six or seven subgenomic mRNAs is formed in cells infected with different isolates of porcine reproductive and respiratory syndrome virus.* J Gen Virol, 1996. **77 (Pt 6)**: p. 1265-70.
28. Tian, K., et al., *Emergence of fatal PRRSV variants: unparalleled outbreaks of atypical PRRS in China and molecular dissection of the unique hallmark.* PLoS One, 2007. **2**(6): p. e526.
29. Karniychuk, U.U., et al., *Pathogenesis and antigenic characterization of a new East European subtype 3 porcine reproductive and respiratory syndrome virus isolate.* BMC Vet Res, 2010. **6**: p. 30.
30. Christianson, W.T., et al., *Experimental reproduction of swine infertility and respiratory syndrome in pregnant sows.* Am J Vet Res, 1992. **53**(4): p. 485-8.
31. Collins, J.E., et al., *Isolation of swine infertility and respiratory syndrome virus (isolate ATCC VR-2332) in North America and experimental reproduction of the disease in gnotobiotic pigs.* J Vet Diagn Invest, 1992. **4**(2): p. 117-26.
32. Pejsak, Z., T. Stadejek, and I. Markowska-Daniel, *Clinical signs and economic losses caused by porcine reproductive and respiratory syndrome virus in a large breeding farm.* Vet Microbiol, 1997. **55**(1-4): p. 317-22.

33. Young, B., et al., *Clinical signs and their association with herd demographics and porcine reproductive and respiratory syndrome (PRRS) control strategies in PRRS PCR-positive swine herds in Ontario.* Can J Vet Res, 2010. **74**(3): p. 170-7.
34. Rossow, K.D., et al., *Experimental porcine reproductive and respiratory syndrome virus infection in one-, four-, and 10-week-old pigs.* J Vet Diagn Invest, 1994. **6**(1): p. 3-12.
35. Esch, G., et al., *Parasitism: The Diversity and Ecology of Animal Parasites.* Parasitology, 2001. **123**.
36. Albina, E., *Epidemiology of porcine reproductive and respiratory syndrome (PRRS): an overview.* Vet Microbiol, 1997. **55**(1-4): p. 309-16.
37. Christianson, W.T., et al., *Pathogenesis of porcine reproductive and respiratory syndrome virus infection in mid-gestation sows and fetuses.* Can J Vet Res, 1993. **57**(4): p. 262-8.
38. Bierk, M.D., et al., *Transmission of porcine reproductive and respiratory syndrome virus from persistently infected sows to contact controls.* Can J Vet Res, 2001. **65**(4): p. 261-6.
39. Otake, S., et al., *Transmission of porcine reproductive and respiratory syndrome virus by needles.* Vet Rec, 2002. **150**(4): p. 114-5.
40. Dee, S., J. Deen, and C. Pijoan, *Evaluation of 4 intervention strategies to prevent the mechanical transmission of porcine reproductive and respiratory syndrome virus.* Can J Vet Res, 2004. **68**(1): p. 19-26.
41. Music, N. and C.A. Gagnon, *The role of porcine reproductive and respiratory syndrome (PRRS) virus structural and non-structural proteins in virus pathogenesis.* Anim Health Res Rev, 2010. **11**(2): p. 135-63.
42. Kappes, M.A. and K.S. Faaberg, *PRRSV structure, replication and recombination: Origin of phenotype and genotype diversity.* Virology, 2015. **479-480**: p. 475-86.
43. Dokland, T., *The structural biology of PRRSV.* Virus Res, 2010. **154**(1-2): p. 86-97.
44. Bloemraad, M., et al., *Porcine reproductive and respiratory syndrome: temperature and pH stability of Lelystad virus and its survival in tissue specimens from viraemic pigs.* Vet Microbiol, 1994. **42**(4): p. 361-71.
45. Xue, B., et al., *Do Viral Proteins Possess Unique Features?*, in *Flexible Viruses*. 2011. p. 1-34.
46. Slonczewski, J. and J.W. Foster, *Microbiology : an evolving science*. 2017.
47. Wu, W.H., et al., *The 2b protein as a minor structural component of PRRSV.* Virus Res, 2005. **114**(1-2): p. 177-81.
48. Oh, J. and C. Lee, *Proteomic characterization of a novel structural protein ORF5a of porcine reproductive and respiratory syndrome virus.* Virus Res, 2012. **169**(1): p. 255-63.
49. Li, Y., et al., *Nsp9 and Nsp10 contribute to the fatal virulence of highly pathogenic porcine reproductive and respiratory syndrome virus emerging in China.* PLoS Pathog, 2014. **10**(7): p. e1004216.
50. Nauwynck, H.J., et al., *Entry of porcine reproductive and respiratory syndrome virus into porcine alveolar macrophages via receptor-mediated endocytosis.* J Gen Virol, 1999. **80 (Pt 2)**: p. 297-305.
51. Provost, C., et al., *Identification of a new cell line permissive to porcine reproductive and respiratory syndrome virus infection and replication which is phenotypically distinct from MARC-145 cell line.* Virol J, 2012. **9**: p. 267.

52. Kreutz, L.C., *Cellular membrane factors are the major determinants of porcine reproductive and respiratory syndrome virus tropism.* Virus Res, 1998. **53**(2): p. 121-8.
53. Chen, Y., et al., *Additive inhibition of porcine reproductive and respiratory syndrome virus infection with the soluble sialoadhesin and CD163 receptors.* Virus Res, 2014. **179**: p. 85-92.
54. Tian, D., et al., *Arterivirus minor envelope proteins are a major determinant of viral tropism in cell culture.* J Virol, 2012. **86**(7): p. 3701-12.
55. Prather, R.S., et al., *An intact sialoadhesin (Sn/SIGLEC1/CD169) is not required for attachment/internalization of the porcine reproductive and respiratory syndrome virus.* J Virol, 2013. **87**(17): p. 9538-46.
56. Elle Love Mcluskey, A.A., Paul Digard,Christine Tait-Burkard, *PRRSV entry into porcine alveolar macrophages occurs through macropinocytic or*

phagocytic uptake pathways, in *XVth International Nidovirus Symposium*. 2021: Online event.
57. Delputte, P.L., et al., *IFN-alpha treatment enhances porcine Arterivirus infection of monocytes via upregulation of the porcine Arterivirus receptor sialoadhesin.* J Interferon Cytokine Res, 2007. **27**(9): p. 757-66.
58. Loving, C.L., et al., *Innate and adaptive immunity against Porcine Reproductive and Respiratory Syndrome Virus.* Vet Immunol Immunopathol, 2015. **167**(1-2): p. 1-14.
59. Butler, J.E., et al., *Porcine reproductive and respiratory syndrome (PRRS): an immune dysregulatory pandemic.* Immunol Res, 2014. **59**(1-3): p. 81-108.
60. Du, T., et al., *Antiviral Strategies against PRRSV Infection.* Trends Microbiol, 2017. **25**(12): p. 968-979.
61. Fano, E., L. Olea, and C. Pijoan, *Eradication of porcine reproductive and respiratory syndrome virus by serum inoculation of naïve gilts.* Can J Vet Res, 2005. **69**(1): p. 71-4.
62. Karuppannan, A.K., et al., *Natural compounds inhibiting the replication of Porcine reproductive and respiratory syndrome virus.* Antiviral Res, 2012. **94**(2): p. 188-94.
63. Liu, K., et al., *Antiviral activity of phage display selected peptides against Porcine reproductive and respiratory syndrome virus in vitro.* Virology, 2012. **432**(1): p. 73-80.
64. Gao, L., et al., *Cryptoporus volvatus extract inhibits porcine reproductive and respiratory syndrome virus (PRRSV) in vitro and in vivo.* PLoS One, 2013. **8**(5): p. e63767.
65. Sassu, E.L., et al., *Update on Actinobacillus pleuropneumoniae-knowledge, gaps and challenges.* Transbound Emerg Dis, 2018. **65 Suppl 1**: p. 72-90.
66. Pattison, I.H., D.G. Howell, and J. Elliot, *A haemophilus-like organism isolated from pig lung and the associated pneumonic lesions.* J Comp Pathol, 1957. **67**(4): p. 320-30.
67. Shope, R.E., *PORCINE CONTAGIOUS PLEUROPNEUMONIA. I. EXPERIMENTAL TRANSMISSION, ETIOLOGY, AND PATHOLOGY.* J Exp Med, 1964. **119**(3): p. 357-68.
68. Tobias, T.J., et al., *Transmission of Actinobacillus pleuropneumoniae among weaned piglets on endemically infected farms.* Prev Vet Med, 2014. **117**(1): p. 207-14.
69. Tobias, T.J., et al., *A cohort study on Actinobacillus pleuropneumoniae colonisation in suckling piglets.* Prev Vet Med, 2014. **114**(3-4): p. 223-30.
70. Tobias, T.J., et al., *Association between transmission rate and disease severity for Actinobacillus pleuropneumoniae infection in pigs.* Vet Res, 2013. **44**(1): p. 2.
71. Chiers, K., et al., *Actinobacillus pleuropneumoniae infections in closed swine herds: infection patterns and serological profiles.* Vet Microbiol, 2002. **85**(4): p. 343-52.

72. Klinkenberg, D., et al., *Simulation study of the mechanisms underlying outbreaks of clinical disease caused by Actinobacillus pleuropneumoniae in finishing pigs.* Vet J, 2014. **202**(1): p. 99-105.
73. Stringer, O.W., et al., *Proposal of Actinobacillus pleuropneumoniae serovar 19, and reformulation of previous multiplex PCRs for capsule-specific typing of all known serovars.* Vet Microbiol, 2021. **255**: p. 109021.
74. Beck, M., et al., *RTX toxin genotypes and phenotypes in Actinobacillus pleuropneumoniae field strains.* J Clin Microbiol, 1994. **32**(11): p. 2749-54.
75. Dom, P. and F. Haesebrouck, *Comparative virulence of NAD-dependent and NAD-independent Actinobacillus pleuropneumoniae strains.* Zentralbl Veterinarmed B, 1992. **39**(4): p. 303-6.
76. Frey, J., *Virulence in Actinobacillus pleuropneumoniae and RTX toxins.* Trends Microbiol, 1995. **3**(7): p. 257-61.
77. Jacobsen, M.J., J.P. Nielsen, and R. Nielsen, *Comparison of virulence of different Actinobacillus pleuropneumoniae serotypes and biotypes using an aerosol infection model.* Vet Microbiol, 1996. **49**(3-4): p. 159-68.
78. Xu, Z., et al., *Comparative genomic characterization of Actinobacillus pleuropneumoniae.* J Bacteriol, 2010. **192**(21): p. 5625-36.
79. Sárközi, R., L. Makrai, and L. Fodor, *Identification of a proposed new serovar of Actinobacillus Pleuropneumoniae: Serovar 16.* Acta Vet Hung, 2015. **63**(4): p. 444-50.
80. Yang, W., et al., *Loop-mediated isothermal amplification targeting the apxIVA gene for detection of Actinobacillus pleuropneumoniae.* FEMS Microbiol Lett, 2009. **300**(1): p. 83-9.
81. Dreyfus, A., et al., *Use of recombinant ApxIV in serodiagnosis of Actinobacillus pleuropneumoniae infections, development and prevalidation of the ApxIV ELISA.* Vet Microbiol, 2004. **99**(3-4): p. 227-38.
82. Silversides, D.W., et al., *Investigation of the species origin of the St. Jude Porcine Lung epithelial cell line (SJPL) made available to researchers.* J Virol, 2010. **84**(10): p. 5454-5.
83. Seo, S.H., et al., *Characterization of a porcine lung epithelial cell line suitable for influenza virus studies.* J Virol, 2001. **75**(19): p. 9517-25.
84. Bachvaroff, R.J., G. Klein, and F.T. Rapaport, *Alterations in cell characteristics in relation to malignant transformation.* Transplant Proc, 1979. **11**(1): p. 1055-9.
85. Bachvaroff, R.J., F. Miller, and F.T. Rapaport, *Appearance of cytoskeletal components on the surface of leukemia cells and of lymphocytes transformed by mitogens and Epstein-Barr virus.* Proc Natl Acad Sci U S A, 1980. **77**(8): p. 4979-83.
86. Yates, M.K. and K.L. Seley-Radtke, *The evolution of antiviral nucleoside analogues: A review for chemists and non-chemists. Part II: Complex modifications to the nucleoside scaffold.* Antiviral Res, 2019. **162**: p. 5-21.
87. Rodwell, V.W., Botham, K. M., Kennelly, P. J., Weil, P. A., & Bender, D. A., *Harper's illustrated biochemistry* 30th ed. 2015, New York: McGraw-Hill Education LLC.
88. Smith, C.M., Marks, A. D., Lieberman, M. A., Marks, D. B., & Marks, D. B., *Marks' basic medical biochemistry: A clinical approach*. 2005, Philadelphia: Lippincott Williams & Wilkins.

89. Seley-Radtke, K.L. and M.K. Yates, *The evolution of nucleoside analogue antivirals: A review for chemists and non-chemists. Part 1: Early structural modifications to the nucleoside scaffold.* Antiviral Res, 2018. **154**: p. 66-86.
90. Zhang, H.W., et al., *Synthesis of purine modified 2'-C-methyl nucleosides as potential anti-HCV agents.* Bioorg Med Chem Lett, 2011. **21**(22): p. 6788-92.
91. Carroll, S.S., et al., *Inhibition of hepatitis C virus RNA replication by 2'-modified nucleoside analogs.* J Biol Chem, 2003. **278**(14): p. 11979-84.
92. Pierra, C., et al., *Synthesis and pharmacokinetics of valopicitabine (NM283), an efficient prodrug of the potent anti-HCV agent 2'-C-methylcytidine.* J Med Chem, 2006. **49**(22): p. 6614-20.
93. Eldrup, A.B., et al., *Structure-activity relationship of heterobase-modified 2'-C-methyl ribonucleosides as inhibitors of hepatitis C virus RNA replication.* J Med Chem, 2004. **47**(21): p. 5284-97.
94. Eldrup, A.B., et al., *Structure-activity relationship of purine ribonucleosides for inhibition of hepatitis C virus RNA-dependent RNA polymerase.* J Med Chem, 2004. **47**(9): p. 2283-95.
95. Franchetti, P., et al., *Antitumor activity of C-methyl-beta-D-ribofuranosyladenine nucleoside ribonucleotide reductase inhibitors.* J Med Chem, 2005. **48**(15): p. 4983-9.
96. Orlov, A.A., et al., *New tools in nucleoside toolbox of tick-borne encephalitis virus reproduction inhibitors.* Bioorg Med Chem Lett, 2017. **27**(5): p. 1267-1273.
97. Koole, L.H., et al., *Conformation of two 4'-thio-2'-deoxynucleoside analogs studied by 5000-MHz proton NMR spectroscopy and x-ray crystallography.* Journal of the American Chemical Society, 1992. **114**(25): p. 9936-9943.
98. Waga, T., et al., *Synthesis of 4'-C-Methylnucleosides.* Bioscience, Biotechnology, and Biochemistry, 1993. **57**(9): p. 1433-1438.
99. Cameron, C.E. and C. Castro, *The mechanism of action of ribavirin: lethal mutagenesis of RNA virus genomes mediated by the viral RNA-dependent RNA polymerase.* Curr Opin Infect Dis, 2001. **14**(6): p. 757-64.
100. Jordheim, L.P., et al., *Advances in the development of nucleoside and nucleotide analogues for cancer and viral diseases.* Nat Rev Drug Discov, 2013. **12**(6): p. 447-64.
101. Galmarini, C.M., J.R. Mackey, and C. Dumontet, *Nucleoside analogues and nucleobases in cancer treatment.* Lancet Oncol, 2002. **3**(7): p. 415-24.
102. Pertusati, F., M. Serpi, and C. McGuigan, *Medicinal chemistry of nucleoside phosphonate prodrugs for antiviral therapy.* Antivir Chem Chemother, 2012. **22**(5): p. 181-203.
103. McGuigan, C., et al., *Aryl phosphoramidate derivatives of d4T have improved anti-HIV efficacy in tissue culture and may act by the generation of a novel intracellular metabolite.* J Med Chem, 1996. **39**(8): p. 1748-53.
104. McGuigan, C., et al., *Application of phosphoramidate ProTide technology significantly improves antiviral potency of carbocyclic adenosine derivatives.* J Med Chem, 2006. **49**(24): p. 7215-26.
105. De Clercq, E. and J. Neyts, *Antiviral Agents Acting as DNA or RNA Chain Terminators*, in *Antiviral Strategies*, H.-G. Kräusslich and R. Bartenschlager, Editors. 2009, Springer Berlin Heidelberg: Berlin, Heidelberg. p. 53-84.
106. Deval, J., *Antimicrobial Strategies.* Drugs, 2009. **69**(2): p. 151-166.

107. Mehellou, Y., H.S. Rattan, and J. Balzarini, *The ProTide Prodrug Technology: From the Concept to the Clinic.* Journal of Medicinal Chemistry, 2018. **61**(6): p. 2211-2226.
108. Siegel, D., et al., *Discovery and Synthesis of a Phosphoramidate Prodrug of a Pyrrolo[2,1-f][triazin-4-amino] Adenine C-Nucleoside (GS-5734) for the Treatment of Ebola and Emerging Viruses.* Journal of Medicinal Chemistry, 2017. **60**(5): p. 1648-1661.
109. Lo, M.K., et al., *GS-5734 and its parent nucleoside analog inhibit Filo-, Pneumo-, and Paramyxoviruses.* Sci Rep, 2017. **7**: p. 43395.
110. Sheahan, T.P., et al., *Broad-spectrum antiviral GS-5734 inhibits both epidemic and zoonotic coronaviruses.* Science Translational Medicine, 2017. **9**(396): p. eaal3653.
111. Warren, T.K., et al., *Therapeutic efficacy of the small molecule GS-5734 against Ebola virus in rhesus monkeys.* Nature, 2016. **531**(7594): p. 381-385.
112. Eyer, L., et al., *Nucleoside analogs as a rich source of antiviral agents active against arthropod-borne flaviviruses.* Antivir Chem Chemother, 2018. **26**: p. 2040206618761299.
113. Wills, R.W., et al., *Duration of infection and proportion of pigs persistently infected with porcine reproductive and respiratory syndrome virus.* J Clin Microbiol, 2003. **41**(1): p. 58-62.
114. Allende, R., et al., *Porcine reproductive and respiratory syndrome virus: description of persistence in individual pigs upon experimental infection.* J Virol, 2000. **74**(22): p. 10834-7.
115. Murtaugh, M.P. and M. Genzow, *Immunological solutions for treatment and prevention of porcine reproductive and respiratory syndrome (PRRS).* Vaccine, 2011. **29**(46): p. 8192-204.
116. Thanawongnuwech, R. and S. Suradhat, *Taming PRRSV: revisiting the control strategies and vaccine design.* Virus Res, 2010. **154**(1-2): p. 133-40.
117. Storgaard, T., M. Oleksiewicz, and A. Bøtner, *Examination of the selective pressures on a live PRRS vaccine virus.* Arch Virol, 1999. **144**(12): p. 2389-401.
118. Jackson, E.K., *The 2',3'-cAMP-adenosine pathway.* Am J Physiol Renal Physiol, 2011. **301**(6): p. F1160-7.
119. Wiggan, O., et al., *ADF/cofilin regulates actomyosin assembly through competitive inhibition of myosin II binding to F-actin.* Dev Cell, 2012. **22**(3): p. 530-43.
120. Palumbo, A.M., et al., *Tandem mass spectrometry strategies for phosphoproteome analysis.* Mass Spectrom Rev, 2011. **30**(4): p. 600-25.
121. Englert, M., et al., *Aminoacylation of tRNA 2'- or 3'-hydroxyl by phosphoseryl- and pyrrolysyl-tRNA synthetases.* FEBS Lett, 2013. **587**(20): p. 3360-4.
122. Kamtekar, S., et al., *Toward understanding phosphoseryl-tRNACys formation: the crystal structure of Methanococcus maripaludis phosphoseryl-tRNA synthetase.* Proc Natl Acad Sci U S A, 2007. **104**(8): p. 2620-5.
123. Carlson, B.A., et al., *Identification and characterization of phosphoseryl-tRNA^{[Ser]Sec} kinase.* Proceedings of the National Academy of Sciences of the United States of America, 2004. **101**(35): p. 12848-12853.
124. Long, S., et al., *Fatty Acids Regulate Porcine Reproductive and Respiratory Syndrome Virus Infection via the AMPK-ACC1 Signaling Pathway.* Viruses, 2019. **11**(12).